Scholars' Mine

Summer 2016

Carbon transfer from magnesia-graphite ladle refractories to ultra-low carbon steel

Andrew Arthur Russo

CARBON TRANSFER FROM MAGNESIA-GRAPHITE LADLE REFRACTORIES

TO ULTRA-LOW CARBON STEEL

by

ANDREW ARTHUR RUSSO

A THESIS

Presented to the Faculty of the Graduate School of the

MISSOURI UNIVERSITY OF SCIENCE AND TECHNOLOGY

In Partial Fulfillment of the Requirements for the Degree

MASTER OF SCIENCE IN METALLURGICAL ENGINEERING

2016

Approved by

Jeffrey D. Smith, Co-advisor
Von L. Richards Co-advisor
Ronald J. O'Malley

PUBLICATION THESIS OPTION

This thesis is composed of two manuscripts prepared for conference proceedings. Pages 3–28 have been prepared in the style utilized by AIST for presentation at AISTech 2016. Pages 29–46 have been prepared for presentation at ACerS' 52nd St. Louis section symposium. Appendix A and Appendix B have been added to supplement the thesis.

ABSTRACT

Ultra-low carbon steels are utilized in processes which require maximum ductility. Increases in interstitial carbon lower the ductility of steel; therefore, it is important to examine possible sources of carbon. The refractory ladle lining is one such source. Ladle refractories often contain graphite for its desirable thermal shock and slag corrosion resistance. This graphite is a possible source of carbon increase in ultra-low carbon steels. The goal of this research is to understand and evaluate the mechanisms by which carbon transfers to ultra-low carbon steel from magnesia-graphite ladle refractory.

Laboratory dip tests were performed in a vacuum induction furnace under an argon atmosphere to investigate these mechanisms. Commercial ladle refractories with carbon contents between 4-12 wt% were used to investigate the effect of refractory carbon content. Slag-free dip tests and slag-containing dip tests with varying MgO concentrations were performed to investigate the influence of slag. Carbon transfer to the steel was controlled by steel penetrating into the refractory and dissolving carbon in dip tests where no slag was present. The rate limiting step for this mechanism is convective mass transport of carbon into the bulk steel. No detectable carbon transfer occurred in dip tests with 4 and 6 wt%C refractories without slag because no significant steel penetration occurred. Carbon transfer was controlled by the corrosion of refractory by slag in dip tests where slag was present.

ACKNOWLEDGMENTS

TABLE OF CONTENTS

LIST OF ILLUSTRATIONS

LIST OF TABLES

NOMENCLATURE

Symbol	Description
ULC	Abbreviation for ultra-low carbon
SEM	Abbreviation for scanning electron microscopy/microscope
EDX	Abbreviation for energy-dispersive x-ray
C_s	Solid carbon
$\underline{C}$	Carbon dissolved in steel
CO_g	Gaseous carbon monoxide
$\underline{O}$	Oxygen dissolved in steel
MgO_s	Solid magnesia
Mg_g	Gaseous magnesium
FeO_{slag}	Iron oxide dissolved in slag
Fe_l	Liquid iron
VIF	Abbreviation for vacuum induction furnace
ID	Abbreviation for inner diameter
UHP	Abbreviation for ultra high purity
SA/V	Ratio of surface area of refractory to volume of steel
r	Pore radius
γ	Surface tension
θ	Wetting angle
P	Ferrostatic pressure
ρ_{steel}	Density of steel

Symbol	Description
h	Steel height
g	Acceleration due to gravity
MgO_{slag}	Magnesia dissolved in slag
dC_C/dt	Dissolution rate of carbon into steel as change in concentration w/ time
dM_C/dt	Dissolution rate of carbon into steel as change in mass with time
A_{CS}	Area of carbon in contact with steel
$a_{\underline{C}}$	Carbon activity in liquid steel
K	Equilibrium constant for carbon dissolution into steel
k	Rate constant for carbon dissolution into steel
a_{solid}	Activity of solid carbon
C_∞	Bulk carbon concentration of steel
β_C	Mass transfer coefficient of carbon into steel
C_{sat}	Saturated carbon concentration of steel
[MgO]	Magnesia concentration of slag
$[MgO]_{sat}$	Saturated magnesia concentration of slag
β_{MgO}	Mass transfer coefficient of magnesia into slag
$d[MgO]/dt$	Dissolution rate of magnesia into slag
A_{MS}	Contact area between magnesia and slag
V_{Sl}	Volume of slag
dx/dt	Corrosion rate of refractory
ρ_{slag}	Density of slag

Symbol	Description
ρ_{ref}	Density of refractory
$[MgO]_0$	Initial magnesia concentration of slag
XRF	Abbreviation for x-ray fluorescence
V_{St}	Volume of steel
C_o	Initial carbon concentration of steel
V_r	Volume of refractory
l	Refractory immersion depth
R	Refractory radius
d	Steel penetration depth

1. INTRODUCTION

Ultra-low carbon steels can experience an increase in carbon content from contact with carbon-containing refractories.[1] Ultra-low carbon steels are more prone to carbon transfer than higher carbon steels because there is a greater driving force for carbon transfer in ultra-low carbon steels.[2] Furthermore, low-carbon steels have a larger contact area for carbon transfer than high-carbon steels because low-carbon steels wet graphite better than high-carbon steels.[2] Carbon transfer is also more detrimental for ultra-low carbon steels because of their stringent carbon specification of less than 50 ppm.[3] Carbon, in the form of graphite, is often added to refractories to increase the slag corrosion resistance and thermal shock resistance of the refractory.[1,4,5,6,7,8] Carbon-containing refractories will often be the most economical and long-lasting option due to these important properties. Therefore, ultra-low carbon steel heats are often processed in ladles lined with carbon-containing refractories in which the steel will be in contact with the refractories throughout the steelmaking process from the degassing step to the completion of the casting step. Carbon transfer into the ultra-low carbon steel can occur throughout this period of contact with the ladle. Carbon increases as high as 30 ppm carbon have been observed in ultra-low carbon heats with an aim of less than 50 ppm total carbon.[3]

Carbon transfer is detrimental to the properties of ultra-low carbon steel and can cause the steel to not meet grade specifications. Ultra-low carbon steels are utilized in processes that require maximum ductility such as drawing and forming operations. Interstitial carbon adds strength, but lowers the ductility of steel; therefore, an increase in an ultra-low carbon steel's carbon content can make it unusable for forming.[9] When a heat of ultra-low carbon steel experiences carbon pickup in industry, the manufacturer

has two options: attempt to remove carbon at a secondary metallurgy station or demote the heat to a different grade. Both options lead to a loss of profit by either losing time to remove the carbon or by changing the steel to a less valuable grade.

Because of the widespread industrial use of magnesia-carbon refractories in the production of ultra-low carbon steels, the goal of this investigation is to define the controlling kinetic mechanisms and kinetic parameters for carbon transfer from magnesia-graphite ladle refractories to ultra-low carbon steel through experiments which attempt to replicate the conditions of an ultra-low carbon steel in contact with ladle refractory and ladle slag. These goals were accomplished by performing refractory dip tests which a similar ratio of refractory surface area to steel volume seen in a 250 ton industrial ladle. Dip tests were performed within a vacuum induction furnace using an argon atmosphere. Four different magnesia-graphite refractories were tested: 4, 6, 10, and 12 weight percent carbon refractories. Three different slag conditions were used in the dip tests: no slag, low-magnesia slag, and high-magnesia slag.

PAPER

I. Mechanism for Carbon Transfer from Magnesia-Graphite Ladle Refractories to Ultra-Low Carbon Steel

Andrew A. Russo, Jeffrey D. Smith, Ronald J. O'Malley, Von L. Richards

Department of Materials Science and Engineering

Missouri University of Science and Technology

Rolla, MO 65409

ABSTRACT

Mechanisms of carbon transport between magnesia-graphite ladle refractories and ultra-low carbon (ULC) steel were investigated using laboratory dip tests with commercial ladle refractories in a vacuum induction furnace. Refractories with carbon contents between 4-12 wt% were evaluated to observe the effect of carbon content on the rate of carbon transfer to the steel. The influence of slag was also examined by comparing slag free experiments with experiments performed with industrial slag compositions of varying MgO content. The reacted refractories were examined by SEM-EDX analysis to observe changes in the refractory that influenced the rate of carbon pickup to the steel. The mechanism for carbon transfer when refractories of 10 wt%C and 12 wt%C were in contact with ULC steel without slag was dissolution of carbon by steel penetrating into the refractory. There was no penetration and no carbon pickup when 4 wt%C and 6 wt%C refractories were in contact

with ULC steel without slag. The presence of slag changed the pickup mechanism to corrosion of the refractory at the slag line. A slag closer to MgO saturation lessened the extent of that corrosion.

INTRODUCTION

ULC steels are used in processes where maximum ductility is required such as forming and drawing operations, given that interstitial carbon adds strength, but lowers ductility.[1] ULC steels are classified as steels having less than 50 ppm carbon.[2] This strict requirement for carbon requires that carbon transfer from outside sources into the steel must be controlled to ensure that carbon remains within specification. Amavis reports on a French steel plant which had 20-30 ppm pickup when the aim carbon was less than 50 ppm.[2] Outside sources of carbon include alloying additions, electrodes, mold powders, tundish fluxes, and refractories.[1,2,3] Ladle refractories often contain carbon in the form of graphite. Graphite is used because it gives the refractory excellent resistance to corrosion from molten slag, it has good wear resistance and strength at high temperature, it has a low density, and it has excellent resistance to thermal shock.[4,5,6,7,8,9] The negative aspects of using carbon containing refractories are wear by decarburization, skull formation and temperature loss from high thermal conductivity, carbon monoxide corrosion of safety lining, and carbon pickup.[4] Steels with less carbon, such as ULC steels, have greater carbon pickup because there is a greater driving force for carbon transfer to the steel.[10] Also, lower carbon steels wet graphite better than higher carbon steels, so there is added contact area for carbon pickup to occur with lower carbon steels.[10] ULC steels remain in contact with carbon containing refractories from the degassing step to the completion of the casting step in the

steelmaking process and, therefore, are subject to carbon pickup throughout this period of contact with the ladle.

The mechanisms by which carbon transports from refractory to steel must be understood so that they may be controlled. Carbon in contact with steel can be directly dissolved into the liquid steel.

$$C_S \rightarrow \underline{C} \tag{1}$$

Carbon contact with steel can be increased by penetration of steel into carbon containing refractories and by corrosion of the refractory oxides. Another path for carbon transport into steel is the dissociation of carbon monoxide.

$$CO_g \rightarrow \underline{C} + \underline{O} \tag{2}$$

Carbon monoxide can form from carbothermic reduction of refractory oxides such as MgO or through reactions with oxides in slag, such as FeO and MnO.

$$MgO_s + C_s \rightarrow Mg_g + CO_g \tag{3}$$

$$FeO_{slag} + C_s \rightarrow Fe_l + CO_g \tag{4}$$
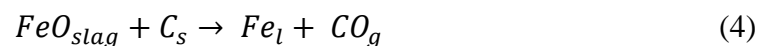
According to the literature, carbon dissolution is the most significant contribution of carbon pickup from ladle refractories.[2,5,11] Carbon dissolution into steel has two steps. First, carbon must dissociate from its base structure and enter the liquid steel at the steel-carbon interface. Then, mass transfer must occur to transport the carbon from the interface into the bulk liquid steel. Many investigators have observed that mass transfer is the rate limiting step for carbon dissolution into molten steel.[7,12,13,14,15,16,17] Jansson *et al.* found carbon pickup from MgO-C refractory during a three hour rotary dip test in ULC Al-killed steel was greatly dependent on convection; C pickup was 0.008 wt% at 0 rpm rotational speed and 0.179 wt% at 800 rpm.[17] Khanna *et al.* found that the dissociation of carbon from its structure may be rate controlling at first, but the reaction speeds up quickly to make mass transfer rate controlling.[12]

Steel penetration can increase contact between steel and graphite in refractories. Khanna *et al.* found that a drop of iron placed on an Al_2O_3-10 wt%C specimen in an argon atmosphere for three hours penetrated 1.5 mm and picked up 5000 ppm carbon.[6] Refractory oxides are normally nonwetting to steel. Thus, an increase in oxide content can limit steel-graphite contact by limiting penetration.[15,18] A decarburized layer at the refractory surface can also prevent steel from contacting carbon in MgO-C refractories when the remaining pore size is small and the steel is nonwetting to MgO. Bannenberg found that carbon pickup was 275 ppm on the first dip of a 3.8 wt%C dolomite refractory rod into steel and only 25 ppm on the second dip due to decarburized layer formation.[20]

Magnesium vapor reacting with oxygen at the refractory steel interface can prevent carbon pickup by creating a dense MgO barrier layer between steel and carbon. Unkilled steel in contact with MgO-C refractory shows continuous growth of a dense MgO layer in the refractory because oxygen is readily available to oxidize the Mg vapor generated by the carbothermic reduction of MgO within the refractory.[5] As a result, unkilled steel picks up carbon quickly at first and then carbon pickup stops once a dense MgO layer develops.[5] Al-killed steel in contact with MgO-C refractory shows rapid growth of a dense MgO layer initially, but the layer ceases to grow later due to a lack of available oxygen.[5] As a result, carbon pickup in Al-killed steel is rapid at first and then slows. Carbon pickup does not stop completely because the dense MgO layer is not continuously regenerated and cracks in the dense layer allow some contact between graphite and steel.[5]

Potschke proposed that CO gas evolution from the reaction of MgO and carbon within the refractory blocks contact between graphite and steel in unkilled steels by preventing steel penetration. However, Lehmann *et al.* only observed a dense layer and no CO bubbling in their experiments.[5] In contrast, Mukai *et al.* observed that bubble formation increased refractory corrosion and that Al additions limited gas bubble formation.[21] Aksel'rod *et al.* observed that carbon in the refractory prevented metal penetration by providing a physical barrier and by creating CO bubbles and gaseous oxide reaction products which limited the wetting of steel to graphite.[22]

Slag infiltration can prevent steel from contacting carbon to inhibit carbon pickup.[19,20] However, slag can also corrode MgO grains in the refractory and lead to exposure of

graphite, which can then dissolve into steel.[23,21] Thus, some carbon pickup can be directly correlated to refractory wear.[2,23] Slag wets the refractory to dissolve the oxide and steel then wets and dissolves the exposed graphite.[10,21,24] Dissolution of MgO into the slag has been identified as the rate controlling step for refractory erosion in the presence of slag. Therefore, increasing the resistance of MgO to slag attack and reducing contact between slag and MgO can limit corrosion.[10,11,21,25] Akkurt found that decreasing wetting between refractory and slag reduced slag corrosion.[9] Refractories that employ larger MgO grains have also been found to exhibit better slag resistance because they have less surface area to attack.[19,26] MgO saturated slags also inhibit dissolution of MgO grains.[9,19,23,27] Basic slags with lower MgO solubility can also limit MgO corrosion.[9,23,28,29] Slag MgO solubility increases with decreasing basicity, increasing alumina, increasing temperature, and increasing FeO.[30] Sintered MgO has been observed to have less slag erosion resistance than fused MgO due to the presence of intergranular silicates which assist slag penetration.[29,33] Porosity, higher temperatures, and longer contact times also increase slag penetration.[31,32,33] Akkurt *et al.* and Resende *et al.* found that increasing carbon content reduces slag attack because carbon limits slag contact with oxide and prevents slag penetration.[9,25,28]

Corrosion of MgO-C refractories is enhanced when slags are strongly stirred.[13,23,34] Stirring enhances the convective mass transport of MgO in the slag. Stirring can also cause erosion of MgO grains and increased penetration of slag in refractories.[34,26] As a result, induction furnace tests can exhibit refractory corrosion rates 3-5 times greater than tests performed in resistance furnaces.[35,26]

While carbon loss by oxidation can inhibit steel penetration, it can also make refractories more susceptible to corrosion through slag infiltration.[1] Oxidation resistance can be increased with less carbon, larger graphite flake size, and lower porosity.[36] A lower partial pressure of oxygen can protect carbon from oxidation. Akkurt *et al.* observed that adding 5 %CO to their Ar atmosphere reduced MgO-C wear by lowering the partial pressure of oxygen.[9]

Carbon transport by CO can occur when CO is created by reduction of refractory or slag oxides by carbon.[19] These reactions are shown in equations 3 and 4. The reduction of MgO by carbon in MgO-C refractories is a significant source of CO.[5] Steel pressure can suppress this reaction on the ladle walls and bottom.[19]

Other methods for controlling carbon pickup have also been reported. Franken *et al.* found that the spread of carbon pickup from carbon containing refractories was too great and unpredictable for use in ULC steels which forced a change to carbon free refractories.[4] Tassot *et al.* switched from 3 wt%C dolomite bricks in the ladle body to 1 wt%C, but the carbon pickup only dropped from 4 ppm to 2 ppm which prompted them to change to carbon-less bricks in the body.[39] Fired dolomite, $MgO-Al_2O_3$, fired spinel, magnesia-chromite, and bauxite refractories have been used to replace carbon containing refractories with some success.[2,3,4,29,39] Other changes can be made that allow the continued use of carbon containing refractories. Low carbon bricks can be decarburized at the hot face and

sintered to form a barrier.[2] Using more corrosion resistant refractory components like ZrO_2 and BN can lower the corrosion rate thereby lowering carbon pickup.[21,40]

Given the wide industry use of MgO-C refractories in the production of ULC steels, the goal of this investigation is to determine the controlling mechanisms for carbon pickup from ladle refractories by performing experiments that attempt to reproduce the conditions present while ULC steel and ladle slag are in contact with the ladle refractory. This was accomplished by conducting refractory dip tests in a vacuum induction furnace (VIF) under an Ar atmosphere using different refractory and slag compositions and ULC steel. The refractories examined were MgO-C with 4 wt%C, 6 wt%C, 10 wt%C, and 12 wt%C. The three heat conditions tested were ULC steel with no slag, ULC steel with slag, and ULC steel with an MgO saturated slag.

PROCEDURE

Materials Preparation

The VIF was relined before each dip test. To reline the furnace, a layer of refractory fiber paper was placed in the furnace. A one inch layer of dry ramming refractory was put at the bottom of the furnace. An alumina crucible with a composition of 89 % alumina, 10 % silica, and 1 % other oxides was placed in the furnace. Dry ram refractory was packed between the alumina crucible and the refractory paper. The furnace was then topped with refractory plastic. The refractory was dried by heat lamp for 12 hours and then preheated by propane torch before the dip test started. Refractory rods were cored from bricks with a 1.27 cm ID core drill bit using water as a lubricant. The wet rods were placed in a drying furnace at 105 ºC. The steel charge chemistry was determined by arc spectroscopy and

LECO carbon and oxygen analysis. The steel was then cleaned of oxide by wire brushing. The slag used was created by mixing commercial oxide powers. The slag chemistry was based on commercial slag compositions for ULC steels. FeO was not included in the slag due to its tendency to oxidize carbon from the steel, which counteracted the carbon pickup measurements. The slag was pre-melted in a graphite crucible at 1350 $^{\circ}$C. The nominal chemistry of the steel and slag starting materials is shown in Table I and Table II.

Table I. Nominal starting chemistry of steel used in dip tests.

	C	Si	Al	Ti	Mn	Cu	Cr	Ni	Mo	Fe
Steel (ppm)	34	237	710	492	737	370	365	407	94	Remainder

Table II. Nominal starting chemistries of slag used in dip tests.

	MgO	Al_2O_3	SiO_2	CaO
Unsaturated Slag (wt%)	7.7	34.7	9.9	47.7
MgO-saturated Slag (wt%)	13.6	32.4	9.3	44.7

Experiment

Refractory dip tests were performed in a VIF to observe the interactions between refractory, steel, and slag. The procedure for the dip test is as follows: A 5.5 kg ULC steel charge was placed in the crucible in the VIF. A no bake sand mold was placed in the pouring area beneath the furnace to collect the steel at the end of the test. A container of Drierite was placed in the chamber to collect any excess moisture. The refractory rod for the dip test was clamped to the end of a maneuverable rod that passed through the top of the VIF chamber. If slag was needed for the test, a pouch made of 1008 steel shim stock containing 110 g slag was placed in the addition cup in Figure 1a. The O-ring of the

chamber door was inspected and cleaned, and the chamber door was closed and sealed. The chamber was evacuated to 67 Pa and then back-filled with ultra high purity (UHP) 99.999 % Ar. The chamber was then evacuated to 67 Pa and refilled with UHP Ar a second time. A steady flow of Ar was maintained during the remainder of the experiment and the flow was monitored by a silicone oil bubbler. The VIF was powered up slowly to melt and heat the charge to an aim temperature of 1600 °C. If slag was needed for the test, it was added and allowed to melt. The temperature was measured using a type-S immersion thermocouple. A pin sample was taken with an evacuated quartz tube just prior to immersion of the refractory rod. The refractory rod was then dipped approximately 3 cm into the melt. After one minute, a pin sample was taken and additional pin samples were then taken every four minutes afterward to 30 minutes. The refractory rod was removed from the melt, and a final temperature reading was taken. The steel was then poured into the mold, and the power to the furnace was shut down. The experimental furnace setup is shown in Figure 1b.
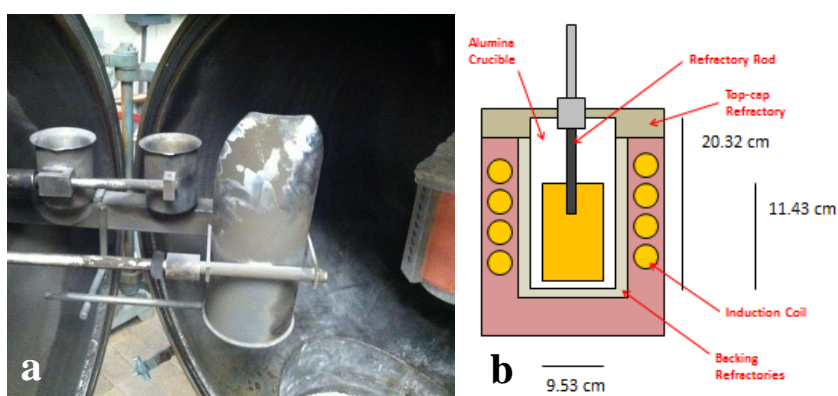
Figure 1. a) VIF chamber with maneuverable containers used to add slag. b) Experimental setup in the VIF.

Analysis

The steel pin samples were analyzed using an arc spectrometer. Pieces weighing between 0.6 and 1 g were cut from the pin samples to measure carbon and oxygen by LECO analyses. The refractory samples were sectioned as shown in Figure 2 and mounted in epoxy. The refractory surface was polished to 1 µm finish using diamond paste. The polished refractory surface was imaged with a digital camera and by optical microscopy. The polished surfaces were then coated by gold palladium. SEM images and EDX maps were obtained using an ASPEX SEM.
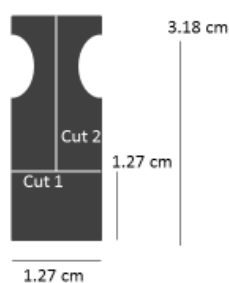
Figure 2. Sectioning refractory dip samples for analysis: Cut 1 was used to observe the refractory in contact with steel. Cut 2 was used to observe the slag line.

RESULTS

Carbon pickup from each dip test is shown in Table III. The SA/V shown in Table III is the surface area of refractory in contact with steel divided by the volume of steel. This value fluctuates due to the variation in refractory immersion depth from the dipping method. The aim immersion depth of 3.2 cm was chosen to give a SA/V comparable to an industrial ladle. The initial carbon content of the steel melt also varies somewhat due to variations in the starting material. There was no carbon pickup from 4 wt%C and 6 wt%C dip tests that were performed without slag. The 4 wt%C carbon heats with slag had

less pickup than the 10 wt%C heats with slag. The 4 wt%C and 10 wt%C heats with slag had less carbon pickup when the slag contained more MgO. The 10 wt%C refractory tests were repeated to show reproducibility.

Table III. Carbon pickup of experimental dip tests.

MgO-C Refractory Wt%C	Steel Wt. (Kg)	SA/V (cm²/cm³)* 1000	Slag MgO Content (wt%)	Initial C (ppm)	C Pickup (ppm)
4	5.55	21	0	30 ± 5	0 ± 6
4	5.60	28	7.7	44 ± 11	25 ± 13
4	5.45	18	13.6	47 ± 7	23 ± 12
6	5.65	19	0	40 ± 5	0 ± 5
10	5.65	17	0	33 ± 6	60 ± 18
10	5.55	18	0	34 ± 4	45 ± 7
10	5.70	20	7.7	49 ± 3	55 ± 11
10	5.55	16	7.7	50 ± 2	51 ± 8
10	5.60	28	9.6	55 ± 3	69 ± 8
10	5.55	15	13.6	43 ± 9	29 ± 10
12	5.90	14	0	34 ± 5	45 ± 8

The 10 wt%C heats show a rapid increase in carbon in the first minute followed by a slower linear increase afterward. This can be seen in Figure 3. The rapid increase during the first minute was found to be linearly dependent on the surface area of graphite, as shown in Figure 4. This suggests that the pickup in the first minute is from the dissolution of exposed graphite near the specimen surface during initial steel contact. If this initial stage of carbon pickup is removed from the data, the carbon pickup trend appears to be very similar for all

10 wt%C refractory dip tests, with the exception of the test with 13.6 wt%MgO slag. This

graph can be seen in Figure 5.
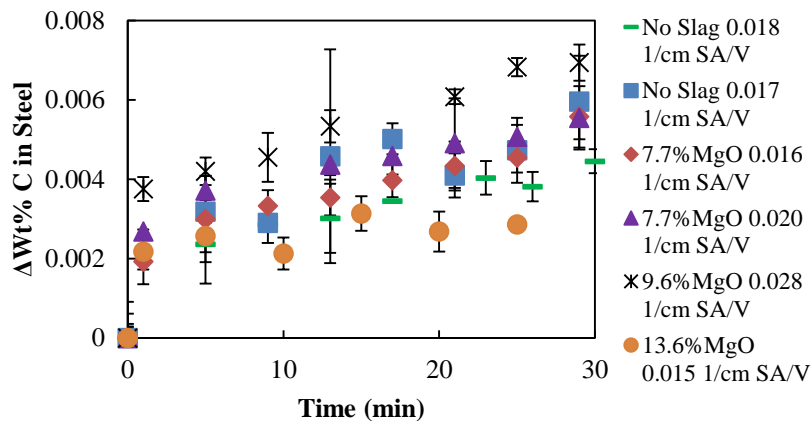
Figure 3. Increase in carbon content of the steel bath vs time for all 10 wt%C refractory tests.
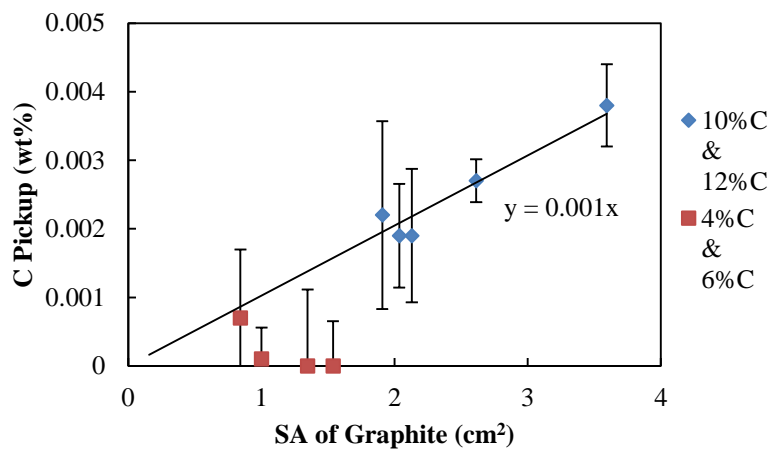
Figure 4. Carbon pickup after the first minute of contact with steel vs area of exposed graphite.
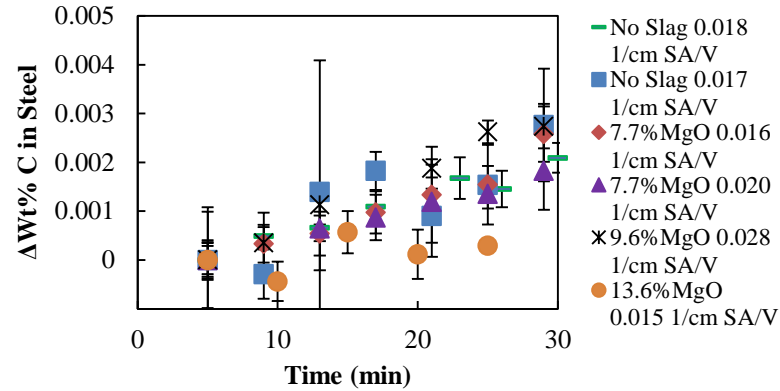
Figure 5. Relative carbon vs time re-zeroed at five minutes of immersion for all 10 wt%C refractory tests.

The 4 wt%C and 6 wt%C dip tests without slag both showed no carbon pickup as shown in Figure 6. Also shown in Figure 6, the 12 wt%C and 10 wt%C samples have a similar carbon pickup trend. This suggests that there is a fundamental change in the mechanism for carbon pickup between high carbon bricks and low carbon bricks.
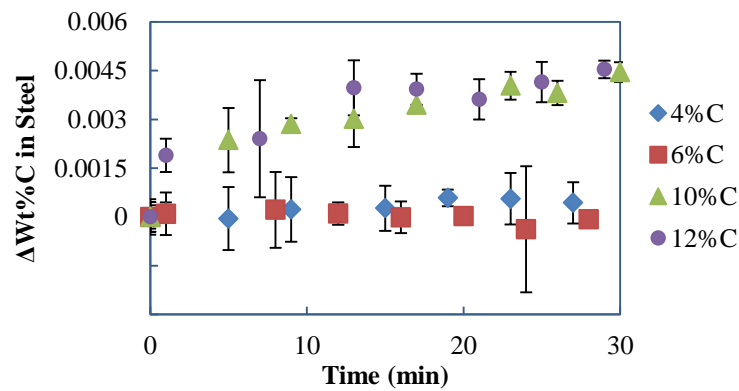
Figure 6. Carbon pickup from MgO-C refractories at 4 different carbon levels from dip tests performed without slag.

The 10 wt%C and the 4 wt%C refractory dip tests that were performed with a 7.7 wt%MgO slag both appear to pick up carbon at the same rate. This can be seen clearly in Figure 7.

The 4 wt%C refractory dip specimen showed much more corrosion at the slag line than the 10 wt%C dip specimen which is why the carbon pickup rate is similar despite the lower carbon content of the 4 wt%C refractory sample. It should be noted that the 4 wt%C refractory dip test does not show the initial large carbon pickup in the first minute that was observed in 10 wt%C refractory dip test.
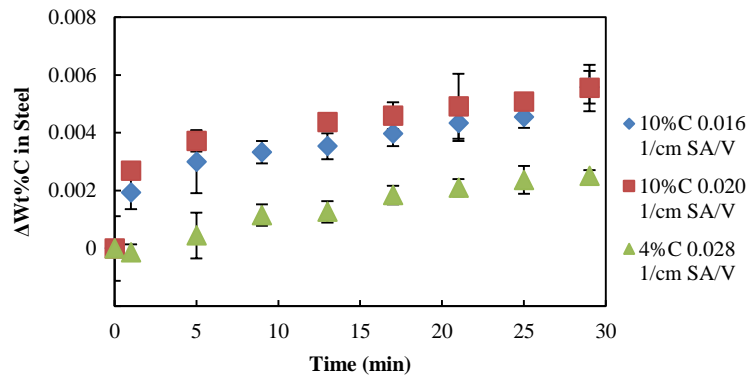
Figure 7. Carbon pickup for 10 wt%C and 4 wt%C refractory dip tests with 7.7 wt%MgO slag.

Dip tests with 13.6 wt%MgO slag showed less corrosion of refractory at the slag line. The 4 wt%C dip test showed an arrest in the carbon pickup at 10 minutes, and the 10 wt%C dip test showed an arrest in the carbon pickup at 15 minutes. The carbon pickup of these dip tests vs time is shown in Figure 8.
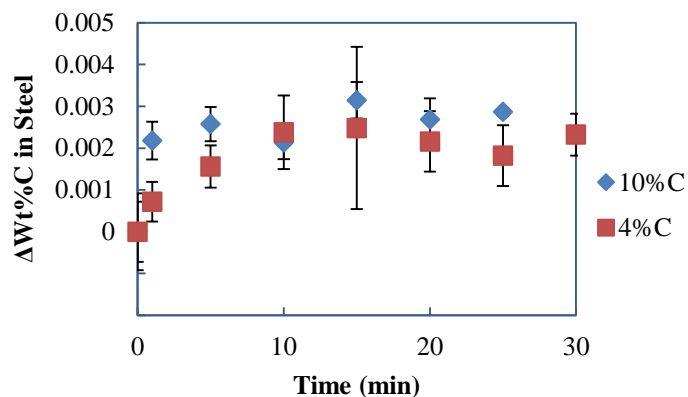
Figure 8. Carbon pickup vs time for 10 wt%C and 4 wt%C dip tests with 13.6 wt%MgO slag.

DISCUSSION

Carbon pickup from 10 wt%C and 12 wt%C refractories can be divided into two stages. The first stage is the rapid increase in carbon seen within the first minute of contact with the steel. The second stage is the slower linear increase of carbon seen in dip tests after the rapid initial pickup. Second stage pickup is seen both with slag and without slag present. The amount of stage one carbon pickup is linearly related to the exposed graphite surface area. This suggests that the source of pickup in the first stage is direct carbon contact at the surface of the refractory that dissolves readily into the steel. An exception to this observed behavior is seen with some 4 wt%C and 6 wt%C refractory samples. Figure 4 indicates that 4 wt%C and 6 wt%C refractory samples generally do not have a carbon pickup consistent with their exposed surface area of graphite. The contact between steel and surface carbon on these samples could be limited by the nonwetting nature of liquid steel to MgO, as Khanna et al. and Ohno et al. have observed.[15,18]

The ability for steel to penetrate the pores of a refractory is dependent on the pore size, pressure and interfacial wetting conditions. The critical radius for steel penetration into the refractory is given by[41]:

$$r = \frac{2\gamma\cos\theta}{\rho_{steel}gh} \tag{6}$$

$$P = \rho_{steel}gh \tag{7}$$

In this equation P is the pressure of the liquid steel, ρ_{steel} is the steel density, h is the bath height, g is the acceleration due to gravity, r is the pore radius, γ is the surface tension of liquid steel and θ is the wetting angle between liquid steel and MgO. For our experiments, the density of liquid steel is 6.98 g/cm^3, the bath height is 3.18 cm, the surface tension for steel (77 ppm oxygen, 90 ppm carbon and 50 ppm sulfur) is 1632 mN/m.[42] and the wetting angle between liquid iron and MgO has been measured to be between 94° and 120°.[43] The pore radius was measured for the 10 wt%C refractory to be between 20 μm and 130 μm and the pore radius for the 4 wt%C refractory was measured to be less than 5 μm. The calculated critical pore radius for refractory penetration by steel, using a wetting angle of θ=94°, is estimated to be about 100 μm for our experiments. Thus, the 10 wt%C refractory that has a pore size greater than the critical pore size can be penetrated by steel and pick up carbon. In contrast, the 4 wt%C refractory with a pore size below the critical pore size is not penetrated by steel and therefore cannot pick up carbon. Figure 9a shows steel penetration observed in a 10 wt%C refractory sample tested with no slag present. No significant steel penetration was observed on the 4 wt%C and 6 wt%C refractory.
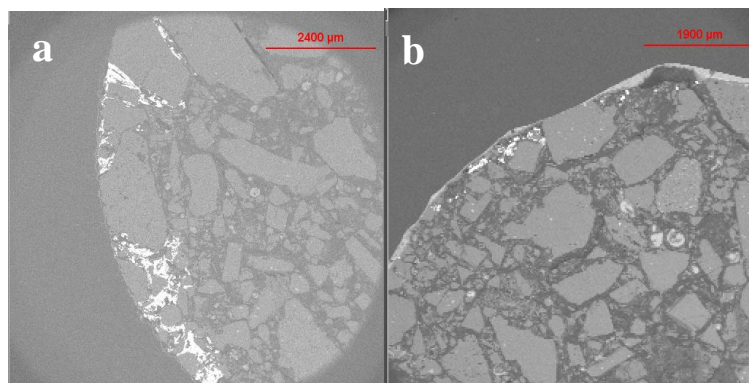
Figure 9. Steel penetration into refractory: (a) 10 wt%C dip test without slag. (b) 10 wt%C dip test with MgO-saturated slag.

The critical pore size calculation suggests that carbon pickup for 10 wt%C and 12 wt%C bricks is controlled by penetration and direct dissolution of graphite when no slag is present. This is in agreement with observations in literature.[2,5,7,12,13,14,15,16,17] No dense MgO layer was observed in our refractory dip test samples. Lehmann *et al.* reported that the growth of a dense MgO layer in MgO-C refractories is inhibited by Al-killing[5], which is in agreement with our findings. The absence of carbon pickup in the 4 wt%C and 6 wt%C refractory dip tests suggest that carbon pickup by a CO transport mechanism is insignificant in our experiments. This is in contrast with the work of Lehmann *et al*. who observed that Al-killed steels increase the driving force for CO transport.[5]

The 4 wt%C and 10 wt%C dip tests performed with a 7.7 wt%MgO slag appear to have the same carbon pickup mechanism because they increase in carbon at the same rate. This would indicate a change in mechanism from steel penetration control in the absence of slag to slag corrosion control when slag is present. All samples in contact with slag experienced some amount of notching at the slag line. Slag dissolves MgO at the slag line and steel

dissolves the exposed graphite.[10,21,24] It can be seen in Figure 9b that steel penetration in 10 wt%C refractory is generally much less when slag is present. It appears that after the surface graphite is dissolved, slag wets the surface of the refractory and inhibits steel penetration. The 10 wt%C refractories still have some steel penetration which influences the rate of carbon pickup. It can be seen in Table IV that the volume corroded decreases significantly when a 10 wt%C refractory is used rather than a 4 wt%C refractory. The volume corroded also decreased for the heats with a 13.6 wt%MgO slag which lowered the observed carbon pickup after 1 minute. The literature confirms that MgO saturated slag decreases corrosion.[9,19,23,27] Thus, corrosion rate of the notch should decrease as slag MgO content approaches saturation. There was still some refractory corrosion in the 13.6 wt%MgO slag heats because corrosion of the alumina crucible during the experiment changed the solubility of MgO in the slag with time. Tayeb *et al.* found that increasing alumina increased the solubility of MgO in slag.[30] Table V shows the initial slag chemistry for the dip tests, the final chemistry of dip test slags, and the MgO needed to saturate the slags. The MgO saturation level was calculated using Factsage® version 7 and FToxid database. The conditions used for the calculations were 1600 ºC and an argon atmosphere with an oxygen partial pressure of 10^{-4}.

Table IV. Calculated carbon pickup of refractory dip tests.

MgO-C Refractory Wt%C	SA/V *1000 (cm²/cm³)	Slag MgO Content (wt%)	C Pickup After 1 min (ppm)	Volume Corroded (cm³)	C Pickup from Corrosion (ppm)	C Pickup from Penetration (ppm)	Calc. C Pickup (ppm)
4	28	7.7	26 ± 5	0.869	19	0	19
4	18	13.6	23 ± 12	0.168	4	27*	31
10	17	0	28 ± 15	0	0	24	24
10	18	0	21 ± 13	0	0	23	23
10	20	7.7	29 ± 8	0.309	15	10	25
10	16	7.7	37 ± 12	0.236	12	5	17
10	28	9.6	32 ± 8	0.207	11	27	38
10	15	13.6	7 ± 5	0.032	2	5	7
12	14	0	26 ± 8	0	0	23	23

*slag penetration

Table V. Final slag compositions of dip tests.

MgO-C Refractory Wt%C	State	MgO (wt%)	Al₂O₃ (wt%)	SiO₂ (wt%)	K₂O (wt%)	CaO (wt%)	TiO₂ (wt%)	FeO (wt%)	MgO Saturation (wt%)
4	Initial	7.70	34.68	9.93	-	47.81	-	-	8.63
	Final	6.08	62.27	4.59	0.10	24.23	2.00	0.64	20.84
4	Initial	13.62	32.41	9.25	-	44.60	-	-	8.64
	Final	11.60	46.88	13.34	0.11	25.21	2.11	0.72	19.43
10	Initial	7.69	34.89	9.96	-	47.75	-	-	8.70
	Final	7.22	55.77	6.19	0.10	28.17	1.94	0.58	18.40
10	Initial	7.70	34.70	9.89	-	47.78	-	-	8.63
	Final	7.13	59.48	4.88	0.11	25.99	1.72	0.62	19.61
10	Initial	9.55	34.00	9.71	-	46.74	-	-	8.65
	Final	9.57	54.69	5.31	0.11	27.23	2.35	0.69	18.62
10	Initial	13.62	32.40	9.25	-	44.63	-	-	8.63
	Final	12.81	51.16	5.23	0.11	27.55	2.42	0.66	17.90

Table IV also shows the calculated carbon pickup based on the amount of penetration and the volume of refractory corrosion. The calculated carbon pickup takes both steel penetration and refractory corrosion into account. The amount of carbon gained through penetration was estimated by calculating the amount of carbon displaced by the penetrated steel in the sample and assuming that all of this carbon entered the steel bath. The amount of carbon from refractory corrosion was estimated by calculating the amount of carbon that was in the corroded volume at the slag line and assuming that all of this carbon entered the steel bath. This volume was calculated by taking the area of the half-ellipse shaped notch in the refractory and multiplying by the circumference of the rod at the centroid of the notch. The calculated pickup is generally in good agreement with the amount of carbon pickup observed in our experiments when the initial pickup by direct contact during the first minute of exposure is excluded, as shown in Figure 10.
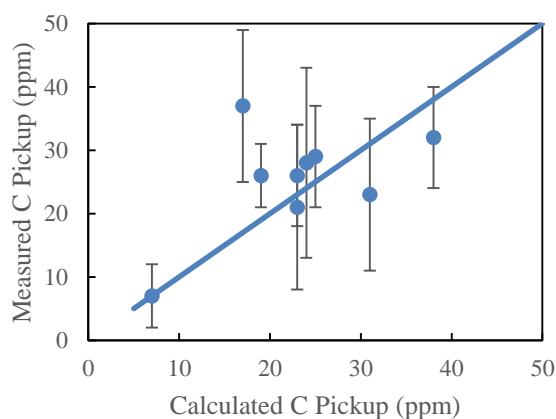
Figure 10. Comparison of calculated and measured carbon pickup from refractory dip tests.

CONCLUSIONS

Laboratory dip tests were performed with industrial MgO-C refractory rod samples in

ULC steel to investigate mechanisms for carbon pickup. The tests showed the effects of

refractory carbon content on the rate of carbon pickup in the presence and absence of

slags with varying MgO content. Four different MgO-C refractories were tested: 4 wt%C,

6 wt%C, 10 wt%C, and 12 wt%C. Three different slag conditions were used: 7.7

wt%MgO, 13.6 wt%MgO, and no slag. The investigation has shown:

- Carbon pickup in the first minute of contact between steel and refractory for 10

  wt%C and 12 wt%C refractories is from the dissolution of graphite near the

  refractory surface by direct contact.

- When no slag is present, carbon pickup after the first minute is controlled by

  penetration of steel into the refractory and dissolution of graphite by the

  penetrating steel for 10 wt%C and 12 wt%C refractories.

- There is no carbon pickup from 4 wt%C and 6 wt%C when there is no slag

  present because the spacing between MgO grains is too small to allow contact

  between steel and graphite or penetration of steel into refractory. MgO-C

  refractories below 6 wt%C are ideal for the barrel and bottom of ladles because of

  their resistance to penetration by steel.

- Carbon pickup is controlled by corrosion of refractory by slag at the slag line for

  dip tests which included slag.

- 4 wt%C refractories showed greater corrosion than 10 wt%C. Thus, MgO-C

  refractories with greater than 10 wt%C are ideal for the slag line of ladles because

  of their resistance to slag corrosion.

- 4 wt%C and 10 wt%C refractories showed less corrosion when the MgO content of the slag was increased. An MgO saturated slag should be employed to minimize slag line erosion.

ACKNOWLEDGMENTS

REFERENCES

1. R. E. Showman and K. E. Lowe, "Controlling Carbon pickup in Steel," *AFS Transactions*, 2010, pp. 385-395.

2. R. Amavis, "3.3 Ultra low carbon," Refractories for the Steel Industry, Springer, 1990, pp. 181-182.

3. C. Jian, Z. Yiyu, Z. Lixin, "Progress of Production Technology of Clean Steel in Baosteel."

4. M. C. Franken, R. Siebring, T. W. M. de Wit, "New Refractory Lining for Steel Ladle BOS' no.2 Corus Ijmuiden," *Unitecr '01,* 2001, pp. 128-138.

5. J. Lehmann, M. Boher, H. Soulard, C. Gatellier, "Metal/Refractory Interactions: A Thermodynamic Approach," *Unitecr '01*, 2001.

6. R. Khanna, M. Ikram-Ul-Haq, Y. Wang, S. Seetharaman, V. Sahajwalla, "Chemical Interactions of Alumina-Carbon Refractories with Molten Steel at 1823K: Implications for Refractory Degradation and Steel Quality," *Metallurgical and Materials Transactions,* Vol. 42B, 2011.

7. R. Khanna, J. Spink, V. Sahajwalla, "Role of Ash Impurities in the Depletion of Carbon from Alumina-Graphite Mixtures in to Liquid Iron," *ISIJ International*, Vol. 47, No. 2, 2007, pp. 282-288.

8. T.J. Wilde. M.R. Hatfield. V.J. Nolan, "Carbon as a Refractory," *Transactions of the American Foundrymen's Society*, Vol. 61, 1953, pp. 640-642.

9. S. Akkurt, H. D. Leigh, "Corrosion of MgO-C Ladle Refractories," *American Ceramic Society Bulletin,* Vol. 82, No. 5, 2003, pp. 32-40.

10. Z. Li, K. Mukai, Z. Tao, "Reactions Between MgO-C Refractory, Molten Slag and Metal," *ISIJ International,* Vol. 40, 2000, pp. S101-S105.

11. J. Poirier, "Impact of Refractory Materials on Industrial Process – Steel Making" *Unitecr '11,* 2011.

12. R. Khanna, F. McCarthy, H. Sun, N. Simento, V. Sahajwalla, "Dissolution of Carbon from Coal-Chars into Liquid Iron at 1550°C," *Metallurgical and Materials Transactions*, Vol. 36B, 2005, pp. 719-729.

13. Y. Shigeno, M. Tokuda, M. Ohtani, "The Dissolution Rate of Graphite into Fe-C Melt Containing Sulphur or Phosphorus," *Transactions of the Japan Institute of Metals*, Vol. 26, No. 1, 1985, pp. 33-43.

14. D. Jang, Y. Kim, M. Shin, and J. Lee, "Kinetics of Carbon Dissolution of Coke in Molten Iron," *Metallurgical and Materials Transactions*, Vol. 43B, 2012, pp. 1308-1314.

15. R. Khanna, B. Rodgers, F. McCarthy, and V. Sahajwalla, "Dissolution of Carbon from Alumina-Carbon Mixtures into Liquid Iron: Influence of Carbonaceous Materials," *Metallurgical and Materials Transactions*, Vol. 37B, pp. 623-632.

16. H. Sun, "Analysis of Reaction Rate Between Solid Carbon and Molten Iron by Mathematical Models," *ISIJ International,* Vol. 45, No. 10, 2005, pp. 1482-1588.

17. S. Jansson, V. Brabie, P. Jönsson, "Magnesia-carbon Refractory Dissolution in Al Killed Low Carbon Steel," *Ironmaking & Steelmaking,* Vol. 33, No. 5, 2006, pp. 389-397.

18. K. Ohno, T. Miyake, S. Yano, C. S. Nguyen, T. Maeda, K. Kunitomo, "Effect of Carbon Dissolution Reaction on Wetting Behavior between Liquid Iron and Carbonaceous Material," *ISIJ International*, Vol. 55, No. 6, 2015, pp. 1252–1258.

19. S. Smets, S. Parada, J. Weytjens, G. Heylen, P.T. Jones, M. Guo, B. Blanpain, P. Wollants, "Behaviour of Magnesia-carbon Refractories in Vacuum-oxygen Decarburisation Ladle Linings," *Ironmaking & Steelmaking*, Vol. 30, No. 4, 2003, pp. 293-300.

20. N. Bannenberg, "Demands on Refractory Material for Clean Steel Production," *Unitecr '95,* 1995.

21. K. Mukai, J. M. Toguri, N. M. Stubina, J. Yoshitomi, "A Mechanism for the Local Corrosion of Immersion Nozzles," *ISIJ International*, Vol. 29, No. 6, 1989, pp. 469-476.

22. L. M. Aksel'rod, O. A. Val'dman, I. Y. Dol'nikov, V. L. Novikov, B. F. Yudin, "Interctions of Steel with Refractories Containing Oxygen Free Additions," *Ogneupory,* No. 10, 1984, pp. 55-58.

23. P. Blumenfeld, S. Peruzzi, M. Puillet, J. de Lorgeril, "Recent Improvements in Arcelor Steel Ladles Through Optimization of Refractory Materials, Steel Shell and Service Conditions," *La Revue de Metallurgie*, 2005.

24. K. Mukai, "Marangoni Flows and Corrosion of Refractory Walls," *Philosophical Transactions: Mathematical, Physical, and Engineering Sciences,* Vol. 356, No. 1739, 1998, pp. 1015-1026.

25. M. Cho, M. V. Ende, T. Eun, I. Jung, "Investigation of Slag-refractory Interactions for the Ruhrstahl Heraeus (RH) Vacuum Degassing Process in Steelmaking," *Journal of the European Ceramic Society*, Vol. 32, 2012, pp. 1503–1517.

26. J. Potschke, C. Bruggmann, "Premature Wear of Refractories due to Marangoni-Convection," *Steel Research International*, Vol. 83, No. 7, 2012, pp. 637-644.

27. H. Sunayama, M. Kawahara, "Corrosion Behavior of MgO-C Refractory Accompanied by Bubble Formation in Molten Slag," *9th Biennial Worldwide Congress on Refractories*, pp. 52-56.

28. W. S. Resende, R. M. Stoll, S. M. Justus, R. M. Andrade, E. Longo, J. B. Baldo, E. R. Leite, C. A. Paskocimas, L. E. B. Soledade, J. E. Gomes, J. A. Varela, "Key Features of Alumina/magnesia/graphite Refractories for Steel Ladle Lining," *Journal of the European Ceramic Society*, Vol. 20, 2000, pp. 1419-1427.

29. S. Parada, M. Guo, P. T. Jones, B. Blanpain, P. Wollants, "Chemical Wear Mechanism of Magnesia-Chromite and Magnesia-Carbon Refractories Exposed to Stainless Steelmaking Slags," *9th Biennial Worldwide Congress on Refractories*, pp. 63-67.

30. M. A. Tayeb, A. N. Assis, S. Sridhar, R. J. Fruehan, "MgO Solubility in Steelmaking Slags," *Metallurgical and Materials Transactions*, Vol. 46B, 2015, pp. 1112-1114.

31. M. Guo, S. Parada, P. T. Jones, J. Van Dyck, E. Boydens, D. Durinck, B. Blanpain, P. Wollants, "Degradation Mechanisms of Magnesia-carbon Refractories by High-alumina Stainless Steel Slags Under Vacuum," *Ceramics International,* Vol. 33, 2007, pp. 1007–1018.

32. M. Guo, S. Parada, P. T. Jones, E. Boydens, J. V. Dyck, B. Blanpain, P. Wollants, "Interaction of Al2O3-rich Slag with MgO–C Refractories During VOD Refining—MgO and Spinel Layer Formation at the Slag/refractory Interface," *Journal of the European Ceramic Society*, Vol. 29, 2009, pp. 1053–1060.

33. L. Musante, P. G. Galliano, E. Brandaleze, V. Muñoz, A. G. T. Martinez, "Chemical Wear of Al_2O_3-MgO-C Bricks by Air and Basic Slags," *Unitecr '13*, 2013, pp. 596-602.

34. X. Li, B. Zhu, T. Wang, "Effect of Electromagnetic Field on Slag Corrosion Resistance of Low Carbon MgO–C Refractories," *Ceramics International*, Vol. 38, 2012, pp. 2105–2109.

35. J. Potschke, T. Deinet, "Premature Corrosion of Refractories by Steel and Slag," *Millenium Steel*, 2005, pp. 109-113.

36. I. Bae, J. No, C. Um, M. Shin, "The Improvement of Casting Ladle Lining for Clean Stainless Steel Production," *Unitecr '07*, 2007.

37. M. Ikram-Ul-Haq, R. Khanna, P. Koshy, V. Sahajwalla, "High-temperature Interactions of Alumina-Carbon Refractories with Molten Iron," *ISIJ International*, Vol. 50, No. 6, 2010, pp. 804-812.

38. M. Y. Solar, R. I. L. Guthrie, "Kinetics of the Carbon-Oxygen Reaction in Molten Iron," *Metallurgical Transactions*, Vol. 3, 1972, pp. 713-722.

39. P. Tassot, D. Verrelle, M. Puillet, "Optimaztion of Refractories of Steel Ladles with Regard to Process Conditions at SOLLAC Dunkirk and Florange."

40. A. Sen, Dr. J. K. Sahu, J. N. Tiwari, "Studies & Optimization of Various Types of Zirconia to Minimize Crack Propagation & Improve Corrosion & Erosion Resistance of Slag Band of Subentry Nozzle," *Unitecr '13*, 2013, pp. 752-757.

41. D. M. Stefanescu, M. D. Owens, A. M. Lane, T. S. Piwonka, K. D. Hayes, J. O. Barlow, "Penetration of Liquid Steel in Sand Molds Part 1: Physics and Chemistry of Penetration and Mathematical Modeling – Metal Side," *AFS Transactions*, 2001.

42. F. A. Halden, W. D. Kinger, "Surface Tension at Elevated Temperatures II Effect of C, N, O, and S on Liquid Iron Surface Tension and Interfacial Effect of C, N, O, and S on Liquid Iron Surface Tension Energy with Al_2O_3, 1955.

43. C. Xuan, H. Shibata, S. Sukenaga, P. G. Jansson, K. Nakajima, "Wettability of Al_2O_3, MgO and Ti_2O_3 by Liquid Iron and Steel," *ISIJ International*, Vol. 55, No. 9, 2015, pp. 1882–1890.

II. Kinetics of Carbon Transfer from Magnesia-Graphite Ladle Refractories to Ultra-Low Carbon Steel

Andrew A. Russo, Jeffrey D. Smith, Ronald J. O'Malley, Von L. Richards

Department of Materials Science and Engineering

Missouri University of Science and Technology

Rolla, MO 65409

ABSTRACT

Kinetic mechanisms of carbon transport to ultra-low carbon (ULC) steel from magnesia-graphite ladle refractories were investigated through laboratory dip tests with commercially available ladle refractories in a vacuum induction furnace. The effect of refractory carbon content on carbon transfer was investigated by using refractories with carbon contents between 4-12 wt%. The influence of slag was also investigated by using slag-free and slag-containing dip tests with varying MgO content. Carbon transfer is controlled by steel penetrating into the refractory and dissolving carbon when no slag is present. The rate controlling step of this mechanism is convective mass transfer of carbon into the bulk steel. The mass transfer coefficient for carbon transfer was found to be approximately $1 \cdot 10^{-6}$ m/s. Corrosion of the refractory controlled the carbon transfer when slag was present. The mass transfer coefficient of MgO into slag was found to be $8 \cdot 10^{-6}$ m/s for 10 wt%C bricks and $12 \cdot 10^{-6}$ m/s for 4 wt%C bricks. The calculated carbon pickup

based on these mechanisms was in good agreement with the measured carbon pickup which supports the proposed mechanisms.

INTRODUCTION

Magnesia-graphite refractories are often employed in ladles to contain molten steel. The graphite in these refractories adds desirable properties such as resistance to molten slag attack, high temperature strength and wear resistance, low density, and thermal shock resistance.[1,2,3,4,5,6] However, the use of graphite has some drawbacks including refractory wear via decarburization, steel skull formation and steel bath temperature loss from graphite's high thermal conductivity, corrosion of the safely lining by reactions with CO, and pickup of carbon by the molten steel.[1] Ultra-low carbon (ULC) steels are particularly sensitive to carbon pickup because there is a greater driving force for carbon transport compared to higher carbon steels.[7] Interstitial carbon increases the strength of steel and decreases the ductility of steel.[8] Carbon pickup is detrimental to the processing of ULC steels because they are employed in forming and drawing operations where ductility must be at a maximum. Thus, the final carbon concentration of ULC steel is specified as less than 50 ppm.[9] Carbon pickup from MgO-C ladle refractories must be controlled to meet this specification. When carbon transfer is out of control, carbon pickup as high as 30 ppm can occur on a ULC steel heat with an aim under 50 ppm carbon.[9]

The kinetics of carbon transfer from refractory to steel should be well understood to control carbon pickup in molten steel. Carbon transfer into molten steel can occur through direct dissolution of graphite.

$$C_S \rightarrow \underline{C} \tag{1}$$

Steel can come into contact with graphite in MgO-C refractories by contact at the surface of the refractory, by steel penetrating into the refractory, and by erosion or corrosion of MgO grains which exposes graphite to steel. The kinetics of MgO transfer into slag should also be well understood if slag corrosion is the controlling mechanism for carbon pickup.

$$MgO_s \rightarrow MgO_{slag} \tag{2}$$

The literature shows that direct dissolution of carbon by steel is the most significant contribution of carbon pickup from ladle refractories.[2,9,10] Two steps have been observed in the direct dissolution of carbon into steel. First, carbon dissolves from its base structure into liquid steel at the interface between steel and carbon. Then, mass transfer of carbon from the steel-carbon interface to the bulk liquid steel occurs.[4,11,12,13,14,15,16] When the interfacial reaction controls the transport of carbon to steel, the dissolution rate can be described by the following equation where $\frac{dM_C}{dt}$ is the dissolution rate of carbon in g/s, A_{CS} is the contact area between steel and carbon in cm^2, a_{solid} is the activity of solid carbon, $a_{\underline{C}}$ is the activity of carbon in the liquid steel, K is the equilibrium constant for carbon dissolution into steel, k is the rate constant of the carbon dissolution reaction in g/(s cm^2).[15]

$$\frac{dM_C}{dt} = A_{CS}k\left(a_{solid} - \frac{a_{\underline{C}}}{K}\right) \tag{3}$$

When convective mass transfer of carbon into the bulk steel controls the transport of carbon, carbon dissolution can be described by the following equation where $\frac{dC_C}{dt}$ is the dissolution rate of carbon as a change in carbon concentration per second, A_{CS} is the area of contact between steel and carbon in m^2, β_C is the mass transfer coefficient in m/s, V_{St} is the volume of the liquid steel in m^3, C_{sat} is the saturation concentration of carbon in steel in wt%, and C_∞ is the carbon concentration of the bulk steel in wt%.[13,15]

$$\frac{dC_C}{dt} = \frac{A_{CS}\beta_C}{V_{St}}(C_{sat} - C_\infty)$$ (4)

Many studies have concluded that mass transfer of carbon into the bulk steel is the rate limiting step for carbon dissolution.[4,11,12,13,14,15,16] However, Khanna *et al.* found evidence suggesting that the interfacial reaction may be rate controlling initially, and the interfacial reaction rate increases quickly which changes rate control to mass transfer.[11]

The corrosion of MgO grains in refractory by slag exposes graphite to dissolution by liquid steel.[17,18] This process begins with slag wetting the refractory and dissolving the exposed oxides. Then, steel wets and dissolves the exposed graphite.[7,17,19] It has been found that dissolution of MgO into slag is the rate controlling step.[7,10,17,20] The dissolution rate of MgO into slag as a change in concentration per second can be described by the following equation where [MgO] is the concentration of MgO in the slag in wt%, [MgO]$_{sat}$ is the concentration of MgO that would saturate the slag in wt%, A_{MS} is the area of contact

between solid MgO and liquid slag in m^2, V_{Sl} is the volume of slag, and β_{MgO} is the mass

transport coefficient of MgO into slag in m/s.[10]

$$\frac{d[MgO]}{dt} = \frac{A_{MS}\beta_{MgO}}{V_{Sl}}([MgO]_{sat} - [MgO]) \tag{5}$$

The dissolution of MgO can also be evaluated through the corrosion rate of the refractory.

The corrosion rate can be described by the following equation where $\frac{dx}{dt}$ is the corrosion

rate in mm/hr, β_{MgO} is the mass transfer coefficient in m/s, ρ_{slag} is the density of the slag in

g/cm^3, ρ_{ref} is the density of the refractory g/cm^3, [MgO]$_{sat}$ is the saturation concentration of

the MgO in the slag in wt%, and [MgO]$_o$ is the initial concentration of the MgO in the slag

in wt%.[21]

$$\frac{dx}{dt} = 36000\beta_{MgO}\frac{\rho_{slag}}{\rho_{ref}}([MgO]_{sat} - [MgO]_0) \tag{6}$$

The goal of this study is to define the controlling kinetic mechanisms and kinetic

parameters for carbon pickup from ladle refractories in ULC steels by analyzing data from

induction furnace dip tests that reflect the conditions present in a ladle of ULC steel. The

effects of different refractories and slag conditions on the kinetic mechanism will also be

observed.

PROCEDURE

Refractory dip tests were performed in a vacuum induction furnace (VIF) under an Ar

atmosphere. The refractory fingers used were cored from commercially available MgO-C

refractories using a 1.27 cm ID core drill bit. Four carbon contents were tested: 4 wt%C, 6 wt%C, 10 wt%C, and 12 wt%C. All dip tests utilized approximately 5.5 kg of ULC steel. The nominal starting chemistry of the steel as shown in Table I was determined by arc spectroscopy. Three different conditions were tested: steel without slag, steel with slag, and steel with MgO saturated slag. The nominal slag chemistries are shown in Table II. These slags were prepared by mixing commercially available oxide powders and pre-melting them in a graphite crucible at 1350 $^{\circ}$C. To begin a dip test, the steel was melted and heated to an aim temperature of 1600 $^{\circ}$C in an alumina crucible with a composition of 89 % alumina, 10 % silica, and 1 % other oxides. Then, slag was added for the experimental runs that required it. An initial pin sample was taken with an evacuated quartz tube. The refractory rod was then submerged approximately 3 cm into the melt. Pin samples were taken one minute after refractory immersion and every four minutes thereafter up to 30 minutes of immersion. More details on the experiment and materials preparation are given in our previous paper.[22]

Table I. Nominal starting chemistry in ppm of ULC steel used in VIF dip tests.

C	Si	Al	Ti	Mn	Cu	Cr	Ni	Mo	Fe
34	237	710	492	737	370	365	407	94	Remainder

Table II. Nominal starting chemistries of slags used in VIF dip tests.

	MgO	Al_2O_3	SiO_2	CaO
Unsaturated Slag (wt%)	7.7	34.7	9.9	47.7
MgO-saturated Slag (wt%)	13.6	32.4	9.3	44.7

The steel pin samples taken from the melt were analyzed using an arc spectrometer. Carbon and oxygen contents of the steel were found by LECO analysis. Post mortem refractory samples were sectioned, mounted in epoxy, and polished to 1 μm finish using diamond paste. The polished refractory surfaces were captured with a digital camera and by optical microscopy. The polished refractory surfaces were coated by gold palladium for SEM imaging and EDX mapping. Post mortem slag samples were analyzed by XRF.

RESULTS AND DISCUSSION

Previous results indicated that carbon pickup was controlled by steel penetration into the refractory when no slag was present.[22] The 4 wt%C and 6 wt%C refractories did not show any carbon pickup when no slag was present because steel could not penetrate the closely packed MgO grains.[22] Carbon pickup was controlled by corrosion of the refractory at the slag line when slag was present in the dip tests.[22] These controlling mechanisms were further evidenced by the agreement between measured carbon pickup values and calculations of expected carbon pickup based on the assumed mechanism.[22]

In the absence of slag, carbon pickup from MgO-C refractories was controlled by the penetration of steel into the refractory. Carbon pickup from penetration of steel into refractory has three steps. First, carbon in front of the penetrating steel is dissolved. Then, carbon diffuses from the high carbon steel at the penetrating tip to the low carbon steel near the interface between the refractory surface and the bulk steel. Finally, mass transfer of carbon into the bulk steel occurs by convection. The carbon concentration profile in the penetrated steel would be different depending on which step was rate limiting as shown in Figure 1. If the carbon dissolution reaction were rate controlling, the penetrating steel and

the bulk steel would have the same carbon content throughout because diffusion and convection transport would occur faster than carbon can be dissolved. By contrast, if diffusion through the penetrating steel were rate controlling, the carbon concentration would steadily decrease from carbon saturation at the penetrating tip to the bulk carbon concentration at the refractory surface because convection would occur fast enough to keep the steel at the refractory surface at the bulk carbon concentration. If convection of carbon into the bulk steel were rate controlling, the penetrated steel would be carbon saturated and a boundary layer would exist between the refractory and bulk steel where the carbon concentration lowers from saturation to the concentration in the bulk. This would occur because the convection of carbon into the bulk would not be able to transport carbon from the refractory surface as fast as diffusion can resupply it.
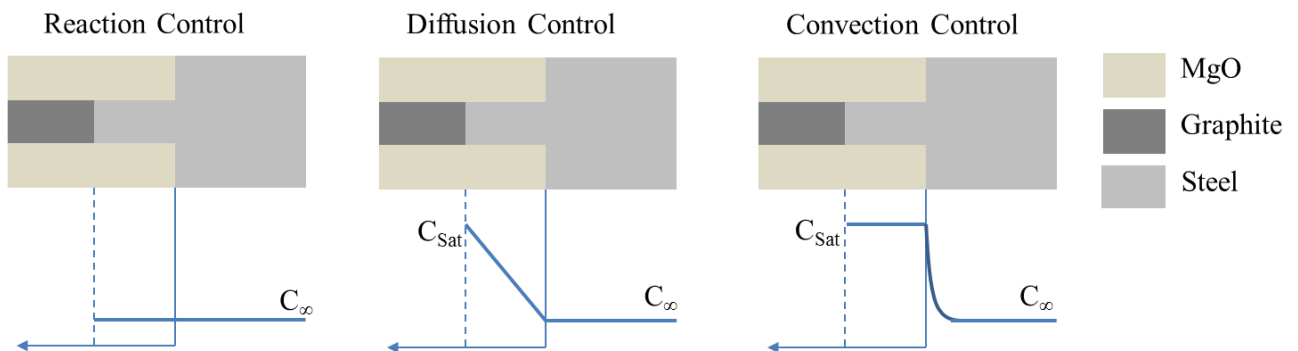
Figure 1. The carbon concentration gradients for three possible rate limiting steps for carbon transport.

A refractory sample from a 10 wt%C heat without slag was etched with 2% nitol solution for 15 seconds to observe the carbon profile of the penetrating steel. Figure 2 shows an optical micrograph of the etched steel. The steel contains massive carbides up to the

refractory surface which suggests that the liquid steel was carbon saturated. This observation suggests that convection is the rate limiting step for carbon pickup by steel penetration.
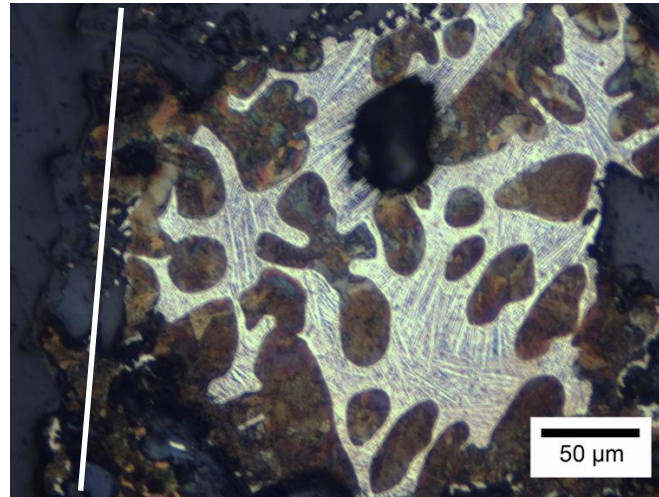
Figure 2. Etched sample of steel penetration in MgO-10 wt%C refractory. The white line is the steel-refractory interface.

The convective mass transfer of carbon into steel described by equation 4 can be integrated to obtain the following equation where C_{sat} is the saturation concentration of carbon in steel in wt%, C_∞ is the carbon concentration of the bulk steel at time t in wt%, C_o is the initial carbon concentration of the steel in wt%, A_{CS} is the area of contact between steel and carbon in m^2, V_{St} is the volume of steel in m^3, and β_C is the mass transfer coefficient in m/s.[15]

$$Ln\left(\frac{C_{sat}-C_\infty}{C_{sat}-C_o}\right) = -\frac{\beta_C A_{CS}}{V_{St}}t \tag{7}$$

Ln((C_{sat}-C_∞)/(C_{sat}-C_o)) was plotted versus time for 10 wt%C and 12 wt%C no slag dip tests as shown in Figure 3. The plots of Ln((C_{sat}-C_∞)/(C_{sat}-C_o)) versus time exhibit linear behavior, providing additional support for convective mass transport of carbon as the rate limiting step. The mass transfer coefficients calculated from Figure 3 were $1.08 \cdot 10^{-6}$ m/s for 10 wt%C 0.017 SA/V, $8.51 \cdot 10^{-7}$ m/s for 10 wt%C 0.018 SA/V, and $1.20 \cdot 10^{-6}$ m/s for 12 wt%C. Carbon pickup data from Jansson et $al.$ gives a value of $1.4 \cdot 10^{-7}$ for $\frac{\beta_C A_{CS}}{V_{St}}$ for dip tests of MgO-5.5 wt%C refractory in ULC steel.[16] This value has reasonable agreement with the $\frac{\beta_C A_{CS}}{V_{St}}$ values shown in Figure 3 given the uncertainties in convection in the two experiments.
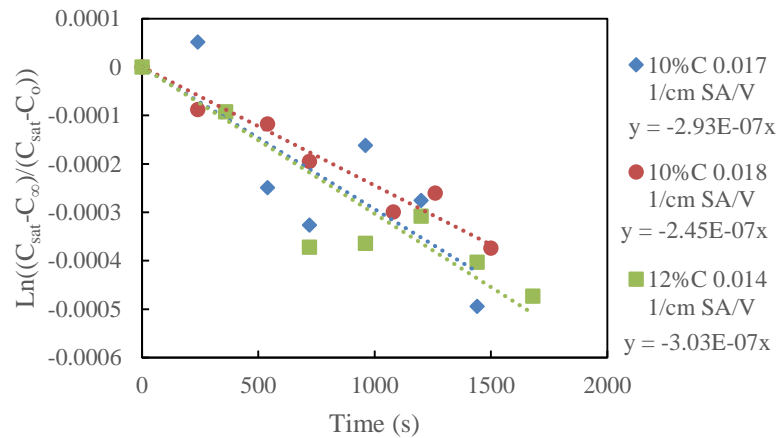
Figure 3. A plot of Ln((C_{sat}-C_∞)/(C_{sat}-C_o)) versus time for dip tests without slag where penetration occurred.

In the presence of slag, refractory corrosion dominates the pickup of carbon. Potschke et $al.$ found that refractory corrosion in an induction furnace containing both steel and slag in contact with refractory can be described by the following equation where $\frac{dx}{dt}$ is the corrosion rate in mm/hr, β_{MgO} is the mass transfer coefficient in m/s, ρ_{slag} is the density of the slag in

g/cm^3, ρ_{ref} is the density of the refractory in g/cm^3, $[MgO]_{sat}$ is the saturation concentration of MgO in the slag in wt%, and $[MgO]_o$ is the initial concentration of MgO in the slag in wt%.[21]

$$\frac{dx}{dt} = 36000\beta_{MgO}\frac{\rho_{slag}}{\rho_{ref}}([MgO]_{sat} - [MgO]_0) \tag{6}$$

Table III shows the initial MgO concentrations and the MgO saturation concentration for the slags used in the dip tests. MgO saturation concentrations were calculated from the final slag chemistries using FactSage® version 7 and FToxid database. The conditions entered into FactSage were 1600 °C and an argon atmosphere with a partial pressure of oxygen of 10^{-4}. The difference between initial slag MgO concentration and MgO saturation was plotted versus the corrosion rate of the refractory dip test fingers in Figure 4. A linear relationship was assumed for simplicity in estimation, but may not represent the actual case. The corrosion rate was calculated from the corrosion notch on post mortem refractory samples and the immersion time. The value of $36000\beta_{MgO}(\rho_{slag}/\rho_{ref})$ is 0.2887 mm/hr for the 10 wt%C dip tests and 0.4797 mm/hr for the 4 wt%C dip tests. Potschke *et al.* calculated this value as 0.24 mm/hr for MgO-C bricks.[21] However, their data showed much scatter because they grouped a range of MgO-C bricks together that had between 5 and 12 wt%C.[21] Their value of 0.24 gives a mass transfer coefficient of $8 \cdot 10^{-6}$ m/s.[21] The mass transfer coefficients calculated from Figure 4 were $8 \cdot 10^{-6}$ m/s for 10 wt%C bricks and $12 \cdot 10^{-6}$ m/s for 4 wt%C bricks. The density of slag was estimated as 2.8 g/cm^3 from collected values of slags similar in temperature and chemistry.[23] The density of the 10 wt%C and 4 wt%C refractories were 2.8 g/cm^3 and 3.1 g/cm^3 respectively.

Table III. Initial MgO content and calculated MgO saturation concentration for dip test slags.

MgO-C Refractory C (wt%)	4	4	10	10	10	10
Initial Slag MgO Content (wt%)	7.70	13.62	7.69	7.70	9.55	13.62
Calculated Slag MgO Saturation (wt%)	21	19	18	20	19	18
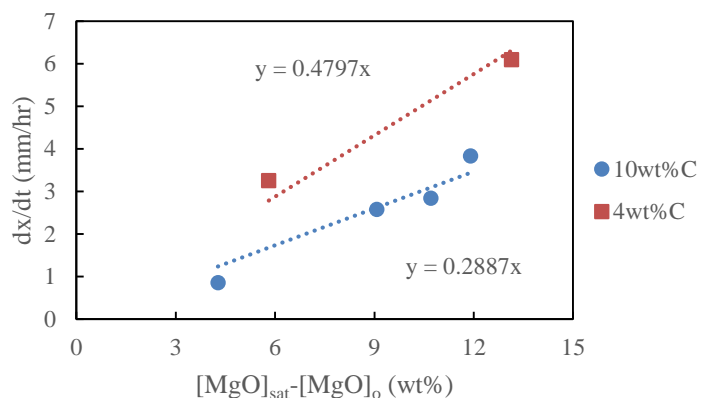
Figure 4. The corrosion rate of refractory dip test fingers versus the difference between MgO saturation and the initial MgO concentration of the slag.

The expected carbon pickup based on the pickup mechanisms revealed above was recalculated for the dip tests. The carbon pickup from penetration was found by analyzing SEM images as shown in Figure 5 of the refractory-steel interface. The images were processed with ImageJ software to measure the area of penetrated steel. This area was multiplied by the submerged length of the refractory rod to obtain a volume. This volume was multiplied by the volume fraction of carbon in the refractory. Then, the weight of carbon in that volume was found. The carbon pickup was calculated by assuming that the volume of steel in the refractory was saturated in carbon and that all the carbon replaced by steel went to either the penetrated steel or the bulk steel.
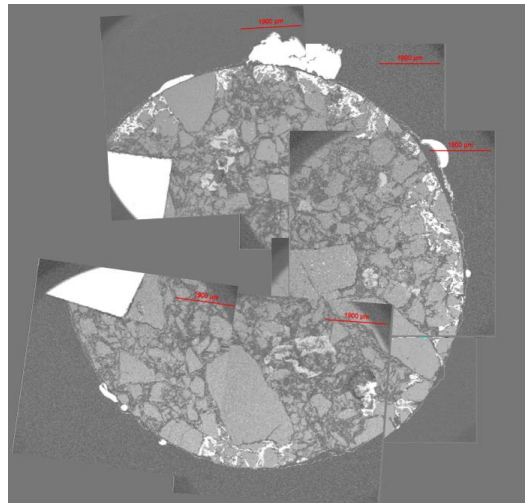
Figure 5. SEM images of 12 wt%C post mortem refractory. Copper tape was placed over an area without steel penetration to maintain conductivity.

Carbon pickup from slag corrosion was estimated by calculating the amount of carbon in the corroded volume at the slag line assuming that all of this carbon entered the steel bath. This volume was calculated by taking the area of the half-ellipse shaped notch at the slag line and multiplying by the circumference of the finger at the centroid of the notch. Figure 6 shows some of the corrosion notches. Table IV shows a comparison of the measured carbon pickup and the calculated carbon pickup for the refractory dip tests. Figure 7 shows that the calculated pickup based on the mechanisms generally agrees well with the measured carbon pickup when measurement error is taken into account.

10 wt%C
7.7 wt%MgO Slag

10 wt%C
13.6 wt%MgO Slag

4 wt%C
7.7 wt%MgO Slag

4 wt%C
13.6 wt%MgO Slag
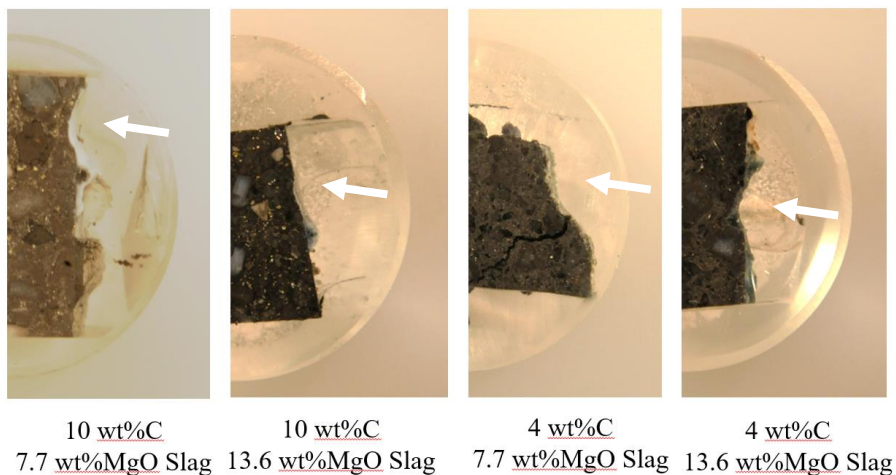
Figure 6. Corrosion notches of refractory fingers. Notches are indicated by white arrows. It can be seen that notch severity decreases with increased graphite in refractory and increased MgO in slag.

Table IV. Measured carbon pickup versus calculated carbon pickup from refractory dip tests.

MgO-C Refractory Wt%C	SA/V*1000 (cm²/cm³)	Slag MgO Content (wt%)	Measured C Pickup (ppm)	Volume Corroded (cm³)	C Pickup from Corrosion (ppm)	C Pickup from Penetration (ppm)	Calc. C Pickup (ppm)
4	28	7.7	26 ± 5	0.87	19	0	19
4	18	13.6	23 ± 12	0.17	4	20*	24
10	17	0	28 ± 15	0	0	44	44
10	18	0	21 ± 13	0	0	31	31
10	20	7.7	29 ± 8	0.31	15	11	26
10	16	7.7	37 ± 12	0.24	12	17	29
10	28	9.6	32 ± 8	0.21	11	21	32
10	15	13.6	7 ± 5	0.032	2	8	10
12	14	0	26 ± 8	0	0	31	31

*Slag Penetration
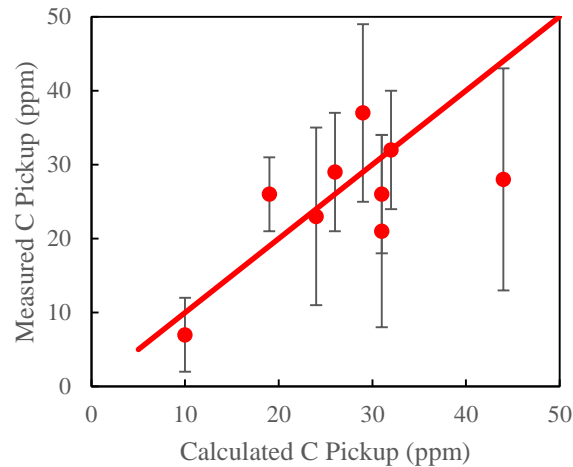
Figure 7. Comparison of the calculated carbon pickup and measured carbon pickup from refractory finger dip tests.

CONCLUSIONS

Refractory finger dip tests have revealed the kinetic mechanisms for carbon pickup in ULC steel. Kinetic parameters have been calculated for these mechanisms and compared with literature values.

- Carbon pickup from 10 wt%C and 12 wt%C refractories is controlled by dissolution of carbon by steel penetrating into the refractory when no slag is present. The rate controlling step for carbon pickup from penetration is convection into the bulk liquid. The mass transfer coefficient for carbon into steel is about $1 \cdot 10^{-6}$ m/s for static dip tests in an induction furnace with no slag.

- Carbon pickup is controlled by slag corrosion of refractory at the slag line for dip tests when slag was present. The controlling mechanism is convective mass transfer of MgO into slag. The mass transfer coefficient of MgO into slag is $8 \cdot 10^{-6}$ m/s for 10 wt%C bricks and $12 \cdot 10^{-6}$ m/s for 4 wt%C bricks for static dip tests in

an induction furnace. The dissolution rate of MgO is slower for bricks with a higher carbon content.

- The measured carbon pickup has been shown to be in reasonable agreement with the carbon pickup calculated based upon the proposed mechanisms for carbon transport to steel.

ACKNOWLEDGMENTS

REFERENCES

1. M.C. Franken, R. Siebring, T.W.M. de Wit, "New Refractory Lining for Steel Ladle BOS' no.2 Corus Ijmuiden," *Unitecr '01,* 2001, pp. 128-138.

2. J. Lehmann, M. Boher, H. Soulard, C. Gatellier, "Metal/Refractory Interactions: A Thermodynamic Approach," *Unitecr '01*, 2001, pp. 23-35

3. R. Khanna, M. Ikram-Ul-Haq, Y. Wang, S. Seetharaman, V. Sahajwalla, "Chemical Interactions of Alumina-Carbon Refractories with Molten Steel at 1823K: Implications for Refractory Degradation and Steel Quality," *Metallurgical and Materials Transactions,* Vol. 42B, 2011, pp. 677-684

4. R. Khanna, J. Spink, V. Sahajwalla, "Role of Ash Impurities in the Depletion of Carbon from Alumina-Graphite Mixtures in to Liquid Iron," *ISIJ International*, Vol. 47, No. 2, 2007, pp. 282-288.

5. T.J. Wilde. M.R. Hatfield. V.J. Nolan, "Carbon as a Refractory," *Transactions of the American Foundrymen's Society*, Vol. 61, 1953, pp. 640-642.

6. S.Akkurt, H.D. Leigh, "Corrosion of MgO-C Ladle Refractories," *American Ceramic Society Bulletin,* Vol. 82, No. 5, 2003, pp. 32-40.

7. Z. Li, K. Mukai, Z. Tao, "Reactions Between MgO-C Refractory, Molten Slag and Metal," *ISIJ International,* Vol. 40, 2000, pp. S101-S105.

8. R.E Showman and K.E. Lowe, "Conrolling Carbon pickup in Steel," *AFS Transactions*, 2010, pp. 385-395.

9. R. Amavis, "3.3 Ultra low carbon," *Refractories for the Steel Industry*, Springer, 1990, pp. 181-182.

10. J. Poirier, "Impact of Refractory Materials on Industrial Process – Steel Making" *Unitecr '11,* 2011, pp. 1-15.

11. R. Khanna, F. McCarthy, H. Sun, N. Simento, V. Sahajwalla, "Dissolution of Carbon from Coal-Chars into Liquid Iron at 1550°C," *Metallurgical and Materials Transactions*, Vol. 36B, 2005, pp. 719-729.

12. Y. Shigeno, M. Tokuda, M. Ohtani, "The Dissolution Rate of Graphite into Fe-C Melt Containing Sulphur or Phosphorus," *Transactions of the Japan Institute of Metals*, Vol. 26, No. 1, 1985, pp. 33-43.

13. D. Jang, Y. Kim, M. Shin, and J. Lee, "Kinetics of Carbon Dissolution of Coke in Molten Iron," *Metallurgical and Materials Transactions*, Vol. 43B, 2012, pp. 1308-1314.

14. R. Khanna, B. Rodgers, F. McCarthy, and V. Sahajwalla, "Dissolution of Carbon from Alumina-Carbon Mixtures into Liquid Iron: Influence of Carbonaceous Materials," *Metallurgical and Materials Transactions*, Vol. 37B, pp. 623-632.

15. H. Sun, "Analysis of Reaction Rate Between Solid Carbon and Molten Iron by Mathematical Models," *ISIJ International,* Vol. 45, No. 10, 2005, pp. 1482-1588.

16. S. Jansson, V. Brabie, P. Jönsson, "Magnesia-carbon Refractory Dissolution in Al Killed Low Carbon Steel," *Ironmaking & Steelmaking,* Vol. 33, No. 5, 2006, pp. 389-397.

17. K. Mukai, J.M. Toguri, N.M. Stubina, J. Yoshitomi, "A Mechanism for the Local Corrosion of Immersion Nozzles," *ISIJ International*, Vol. 29, No. 6, 1989, pp. 469-476.

18. P. Blumenfeld, S. Peruzzi, M. Puillet, J. de Lorgeril, "Recent Improvements in Arcelor Steel Ladles Through Optimization of Refractory Materials, Steel Shell and Service Conditions," *La Revue de Metallurgie*, 2005, pp. 233-239.

19. K. Mukai, "Marangoni Flows and Corrosion of Refractory Walls," *Philosophical Transactions: Mathematical, Physical, and Engineering Sciences,* Vol. 356, No. 1739, 1998, pp. 1015-1026.

20. M. Cho, M. V. Ende, T. Eun, I. Jung, "Investigation of Slag-refractory Interactions for the Ruhrstahl Heraeus (RH) Vacuum Degassing Process in Steelmaking," *Journal of the European Ceramic Society*, Vol. 32, 2012, pp. 1503–1517.

21. J. Potschke, T. Deinet, "Premature Corrosion of Refractories by Steel and Slag," *Millenium Steel*, 2005, pp. 109-113.

22. A. Russo, J. Smith, R. O'Malley, V. Richards, "Mechanism for Carbon Transfer from Magnesia-Graphite Ladle Refractories to Ultra-Low Carbon Steel," *AISTech 2016*, 2016, pp. 1-12, in print.

23. M. Allibert, H. Gaye, J. Geiseler, D. Janke, B. J. Keene, D. Kirner, M. Kowalski, J. Lehmann, K.C. Mills, D. Neuschutz, R. Parra, C. Saint-Jours, P. J. Spencer, M. Susa, M. Tmar, E. Woermann, "Densities of Molten Slags," *Slag Atlas*, Verlag Stahleisen GmbH, Germany, 1995, pp. 313-348.

SECTION

2. CONCLUSIONS

Laboratory dip tests performed with MgO-C refractories in ULC steel revealed important differences in mechanisms for carbon pickup when bricks with different carbon contents and different slag conditions are used.

Dip tests without slag showed a difference in carbon pickup behavior between low carbon 4 & 6 wt%C and high carbon 10 & 12 wt%C bricks. Low carbon bricks showed no significant carbon pickup without slag, but high carbon bricks showed pickup greater than 40 ppm. Carbon pickup in dip tests without slag is from steel penetrating into the refractory and dissolving graphite. Low carbon bricks showed no carbon pickup because the pore size between MgO grains was too small to allow steel penetration. The rate limiting step of carbon pickup without slag was shown to be convective mass transport.

Another significant difference in the carbon pickup behavior between low and high carbon bricks can also be attributed to the pore size. All dip tests with high carbon bricks showed a large increase in carbon pickup during the first minute of immersion. This carbon pickup is from near surface graphite being dissolved.

Carbon pickup behavior is significantly affected by the presence of slag. Low carbon bricks caused carbon pickup at a rate similar to the high carbon bricks in contact with a low MgO slag. Corrosion notches were formed in all dip tests with slag and were more severe in the low carbon refractory. Slag also decreased the amount of penetration

in high carbon dip tests. High MgO slags closer to MgO saturation decreased the amount of corrosion and carbon pickup. Carbon pickup in dip tests with slag is controlled by corrosion of the refractory.

3. FUTURE WORK

3.1 MGO SATURATED SLAG

Conclusions drawn from this paper on MgO slag saturation limiting carbon pickup would be greatly substantiated by dip tests using an MgO crucible and MgO saturated slag to verify that no corrosion and no pickup would occur with low carbon bricks in contact with MgO-saturated slag.

3.2 LINING PREHEAT

Ladle refractories in steel mills are preheated before coming into contact with steel. This causes a decarburized layer to form. The dip tests performed in this work would provide insight into the effect of this layer on carbon pickup. The refractory fingers used could be preheated in air before dip testing to simulate the effect of preheating.

3.3 SPINEL FORMATION

Alumina-Magnesia-Carbon (AMC) refractories are commonly used in the barrel of steel containing ladles. The wetting angle of steel on alumina is greater than the wetting angle of steel on magnesia which should decrease steel penetration. Also, the expansive formation of spinel could prevent penetration. Dip tests with AMC refractories would reveal if they reduce carbon pickup over Magnesia-Carbon refractories by limiting penetration.

3.4 SLAG COATING

When a ladle of ULC steel is being cast, the steel is drained from the bottom of the ladle. This causes a layer of slag to coat the walls of the ladle. The slag layer could

block contact between the steel and refractory which may decrease carbon pickup in the steel. The refractory rods used in this research could be reused after a slag-containing dip test to test the effects of slag coating on carbon pickup.

3.5 THERMAL GRADIENT

Refractories used in an industrial ladle will have a thermal gradient where the refractory face in contact with steel will be hotter than the face in contact with the safety lining. The thermal gradient may affect the carbon pickup by changing the reaction rate of carbon dissolution as the steel penetrates into cooler parts of the refractory. The dip tests performed in this research do not create a significant thermal gradient in the refractory. A refractory crucible test would be able to form a thermal gradient and obtain information on how this gradient affects carbon pickup.

APPENDIX A.

CARBON PICKUP ESTIMATION EXAMPLES

Carbon pickup from penetration was estimated differently in "Mechanism for Carbon Transfer from Magnesia-Graphite Ladle Refractories to Ultra-Low Carbon Steel" than in "Kinetics of Carbon Transfer from Magnesia-Graphite Ladle Refractories to Ultra-Low Carbon Steel." The method for estimating carbon pickup from penetration was changed in the later because the new method more accurately accounts for the amount of steel penetration in the entire observable section of refractory.

In "Mechanism for Carbon Transfer from Magnesia-Graphite Ladle Refractories to Ultra-Low Carbon Steel" the carbon pickup from steel penetration was estimated by measuring an average steel penetration depth (Figure 1) then using that depth to calculate the volume of the tube of refractory where penetration occurred. The fraction of the circumference penetrated was measured (Figure 1). This fraction was multiplied by the volume to find the adjusted volume penetrated. This volume was used to calculate the weight of refractory penetrated. Then, this weight was multiplied by the weight fraction of carbon in the refractory to obtain a weight of carbon. The carbon pickup was estimated by assuming this entire weight went into the bulk steel.
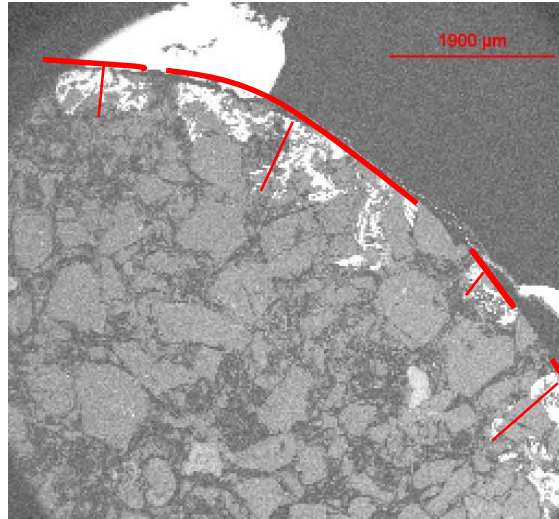
Figure 1. Measurements of penetration depth and surface fraction of penetration.

For example, the average penetration depth for a 10 wt%C dip test was 0.093 cm. The volume of penetration can be described by the following equation where V_r is the volume in cm^3, l is the immersion depth of the refractory finger into the steel in cm, R is the radius of the refractory finger in cm, and d is the steel penetration depth in cm.

$$V_r = \pi l(R^2 - (R - d)^2) + \pi dR^2 \tag{1}$$

The volume of the tube of penetrated refractory for the 10 wt%C dip test was 1.2 cm^3. This was the multiplied by the fraction of the circumference penetration which was 0.4 for the 10 wt%C dip test. The adjusted volume of penetration, therefore, is 0.48 cm^3. This volume is then multiplied by the density of the refractory (2.8 g/cm3) to obtain a refractory weight of 1.4 g. The penetrated weight of refractory is then multiplied by the weight fraction of carbon in refractory (0.1) to obtain a weight of carbon in the penetrated

refractory which is 0.14 g. This weight of carbon was assumed to go in the bulk steel which weighed 5650 g which would make the carbon pickup 24 ppm.

In "Kinetics of Carbon Transfer from Magnesia-Graphite Ladle Refractories to Ultra-Low Carbon Steel" the carbon pickup from steel penetration was estimated by measuring the area of steel penetrated into refractory using image processing software (Figure 2). Then this area was multiplied by the refractory immersion depth to get a volume. This volume was multiplied by the volume fraction of carbon in the refractory. It was assumed that this volume of carbon was completely dissolved by the steel. The volume of steel was assumed to be saturated in carbon. Then, the remaining carbon was assumed to go into the bulk steel.
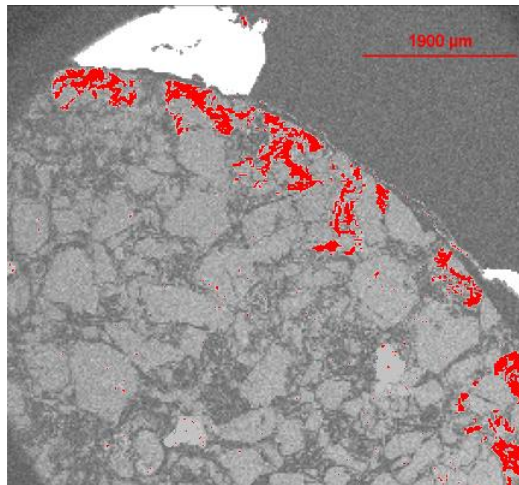
Figure 2. Estimated area of steel penetration from image processing software.

For example, the measured steel penetration area for a 10 wt%C dip test was 0.19 cm^2. This was multiplied by the immersion depth of 3.2 cm to obtain a volume of 0.61 cm^3. Only a certain fraction of this volume would be carbon so this volume was

multiplied by the volume fraction of carbon in the refractory (0.16) to obtain an estimate

of the volume of penetrated steel which was 0.098 cm^3. This volume was assumed to

have displaced an equal volume of carbon. The weight of this volume of carbon was

found by multiplying by the density of graphite (2.16 g/cm^3). The weight of carbon going

into steel was 0.21 g. It was assumed that the penetrated steel was carbon saturated at 5.6

wt%C. The weight of the steel was found by multiplying by the density of steel 6.98

g/cm^3 to obtain 0.68 g. The amount of carbon needed to saturate this steel was 0.038 g.

This left 0.17 g of carbon left to go into the bulk steel which weighed 5550 g. Thus, the

estimated carbon pickup in the bulk was 31 ppm.

Table I shows the values used to estimate carbon pickup from the measured area

of steel penetration for all the dip tests which showed steel penetration.

Table I. Values used to estimate carbon pickup from steel penetration.

MgO-C Refractory Wt%C	Slag Wt% MgO	Penetrated Area (cm^2)	Penetrated Volume (cm^3)	Wt. C (g)	Wt. C to Saturate Steel (g)	Leftover Wt. C (g)	Steel Wt. (kg)	C Pickup from Penetration (ppm)
10	0	0.28	0.14	0.30	0.06	0.25	5.65	44
10	0	0.19	0.10	0.21	0.04	0.17	5.55	31
10	7.7	0.10	0.03	0.07	0.01	0.06	5.70	11
10	7.7	0.13	0.05	0.12	0.02	0.09	5.55	17
10	9.6	0.09	0.07	0.15	0.03	0.12	5.60	21
10	13.6	0.07	0.03	0.05	0.01	0.04	5.55	8
12	0	0.21	0.10	0.22	0.04	0.18	5.90	31

Carbon pickup from slag corrosion in both papers was estimated by calculating

the amount of carbon in the corroded refractory volume at the slag line assuming that all

of this carbon entered the steel bath. This volume was estimated by taking the area of the

half-ellipse shaped notch at the slag line and multiplying by the circumference of the

refractory at the centroid of the notch. Table II shows the measurements and calculations

utilized in calculating the carbon pickup from corrosion.

Table II. Values used to estimate carbon pickup from refractory corrosion.

MgO-C Refractory Wt%C	Slag Wt% MgO	Notch Length (cm)	Notch Depth (cm)	Centroid Position (cm)	Circumference (cm)	Notch Area (cm^2)	Notch Volume (cm^3)	Steel Wt. (kg)	C Pickup from Corrosion (ppm)
4	7.7	1.17	0.29	0.13	3.20	0.27	0.87	5.60	19
4	13.6	0.47	0.13	0.05	3.65	0.05	0.17	5.45	4
10	7.7	0.60	0.14	0.06	3.62	0.06	0.24	5.55	12
10	7.7	0.61	0.23	0.08	3.50	0.09	0.31	5.70	15
10	9.6	0.58	0.12	0.05	3.66	0.06	0.21	5.60	11
10	13.6	0.29	0.04	0.02	3.89	0.01	0.03	5.55	2

APPENDIX B.

DATA TABLES

The ratio of refractory surface area to steel volume for the dip tests was calculated by first calculating the surface area of refractory. The surface area of the refractory in contact with steel was equal to that of a cylinder with a 1.3 cm diameter and a height equal to the refractory immersion depth. Only one of the circular ends of the cylinder was included in the surface area calculation because only one end was in steel contact. The volume of steel was calculated from the weight of steel added to each dip test using the density of liquid steel 6.98 g/cm^3. Table I. shows the values used to calculate the SA/V of each dip test.

Table I. Values used to calculate SA/V for dip tests.

MgO-C Refractory Wt%C	Steel Wt. (kg)	Slag Wt% MgO	Immersion Depth (cm)	SA Refractory (cm^2)	Steel Volume (cm^3)	SA/V*1000 (cm^2/cm^3)
10	5.65	0	3.2	14	809	17
10	5.55	0	3.2	14	795	18
10	5.60	9.6	5.4	22	802	28
10	5.55	13.6	2.7	12	795	15
10	5.55	7.7	2.9	13	795	16
10	5.70	7.7	3.2	16	817	20
12	5.90	0	2.7	12	845	14
4	5.55	0	3.8	17	795	21
4	5.60	7.7	5.4	22	802	28
4	5.45	13.6	3.2	14	781	18
6	5.65	0	3.5	15	809	19

The surface area of graphite in contact with steel, which was plotted against first minute carbon pickup in "Mechanism for Carbon Transfer from Magnesia-Graphite Ladle Refractories to Ultra-Low Carbon Steel", was found by multiplying the surface area of refractory by the volume fraction of graphite in the refractory. Table II shows the values used to make the surface area of graphite versus first minute carbon pickup plot.

Table II. Values used to compare graphite surface area to first minute carbon pickup.

MgO-C Refractory Wt%C	Slag Wt% MgO	Refractory Surface Area (cm^2)	Volume Fraction Graphite	Graphite Surface Area (cm^2)	1st Min. C Pickup (ppm)
4	0	17	0.06	1.0	1±5
4	7.7	22	0.06	1.3	0±11
4	13.6	14	0.06	0.84	7±10
6	0	15	0.10	1.5	0±7
10	9.6	22	0.16	3.6	38±6
10	13.6	12	0.16	1.9	22±14
10	7.7	13	0.16	2.0	19±8
10	7.7	16	0.16	2.6	27±3
12	0	12	0.18	2.1	19±10

Tables III and IV show the measured pore radii of 4 wt%C and 10 wt%C bricks respectively. The 10 wt%C has more measurements because the micrographs of the 10 wt%C brick contained more areas to measure.

Table III. Pore radii measurements between MgO grains of nine locations in 4 wt%C brick (μm).

3.1	1.7	2.3
2.2	2.3	2.3
4.8	4.1	3.1

Table IV. Pore radii measurements between MgO grains of eighteen locations in 10 wt%C brick (μm).

130	110	45	50	77	30
96	37	20	48	34	54
80	47	51	79	49	44

The mass transfer coefficients of carbon into steel without slag were calculated from the values of $\frac{\beta_C A_{CS}}{V_{St}}$ from the kinetic plot. Table V shows the values used to calculate the mass transfer coefficients.

Table V. Values used to calculate the mass transfer coefficient of carbon into steel.

MgO-C Refractory Wt%C	$\dfrac{\beta_C A_{CS}}{V_{St}}$	A_{CS} (cm^2)	V_{St} (cm^3)	β_C (cm/s)
10	2.93E-07	2.2	809	1.08E-04
10	2.45E-07	2.3	795	8.51E-05
12	3.03E-07	2.1	845	1.20E-04

The corrosion rate of the refractories in contact with slag was calculated by dividing the notch depth by the immersion time. The values used to calculate the corrosion rate are shown in Table VI. The plot of corrosion rate against ([MgO]$_{sat}$-[MgO]$_0$) was used to obtain values of $36000\beta_{MgO}(\rho_{slag}/\rho_{ref})$. The mass transfer coefficient of MgO into slag was calculated from these values. Table VII shows the values used to calculate the mass transfer coefficient of MgO into slag.

Table VI. Values used to calculate corrosion rate of refractory.

MgO-C Refractory Wt%C	Slag MgO Wt%	Notch Depth (mm)	Immersion Time (hr)	Corrosion Rate (mm/hr)
4	7.7	2.95	0.48	6.10
4	13.6	1.63	0.50	3.25
10	7.7	1.37	0.48	2.84
10	7.7	1.85	0.48	3.84
10	9.6	1.24	0.48	2.58
10	13.6	0.36	0.42	0.85

Table VII. Values used to calculate mass transfer coefficient of MgO into slag.

MgO-C Refractory Wt%C	$36000\beta_{MgO}(\rho_{slag}/\rho_{ref})$ (mm/hr)	$\beta_{MgO}(\rho_{slag}/\rho_{ref})$ (m/s)	Refractory Bulk Density (g/cm^3)	Slag Density (g/cm^3)	β_{MgO} (m/s)
10	0.2887	8E-6	2.8	2.8	8E-6
4	0.4797	13E-6	3.1	2.8	12E-6

BIBLIOGRAPHY

[1]   M. C. Franken, R. Siebring, T. W. M. de Wit, "New Refractory Lining for Steel Ladle BOS' no.2 Corus Ijmuiden," *Unitecr '01,* 2001, pp. 128-138.

[2]   Z. Li, K. Mukai, Z. Tao, "Reactions Between MgO-C Refractory, Molten Slag and Metal," *ISIJ International,* Vol. 40, 2000, pp. S101-S105.

[3]   R. Amavis, "3.3 Ultra low carbon," Refractories for the Steel Industry, Springer, 1990, pp. 181-182.

[4]   J. Lehmann, M. Boher, H. Soulard, C. Gatellier, "Metal/Refractory Interactions: A Thermodynamic Approach," *Unitecr '01*, 2001.

[5]   R. Khanna, M. Ikram-Ul-Haq, Y. Wang, S. Seetharaman, V. Sahajwalla, "Chemical Interactions of Alumina-Carbon Refractories with Molten Steel at 1823K: Implications for Refractory Degradation and Steel Quality," *Metallurgical and Materials Transactions,* Vol. 42B, 2011.

[6]   R. Khanna, J. Spink, V. Sahajwalla, "Role of Ash Impurities in the Depletion of Carbon from Alumina-Graphite Mixtures in to Liquid Iron," *ISIJ International*, Vol. 47, No. 2, 2007, pp. 282-288.

[7]   T.J. Wilde. M.R. Hatfield. V.J. Nolan, "Carbon as a Refractory," *Transactions of the American Foundrymen's Society*, Vol. 61, 1953, pp. 640-642.

[8]   S. Akkurt, H. D. Leigh, "Corrosion of MgO-C Ladle Refractories," *American Ceramic Society Bulletin,* Vol. 82, No. 5, 2003, pp. 32-40.

[9]   R. E. Showman and K. E. Lowe, "Controlling Carbon pickup in Steel," *AFS Transactions*, 2010, pp. 385-395.

VITA

Andrew Russo was born in St. Louis, MO. He graduated Summa Cum Laude from Missouri University of Science and Technology in May 2014 receiving a Bachelor of Science degree in Metallurgical Engineering. He began working toward a Master of Science degree in Metallurgical Engineering at Missouri University of Science and Technology in the fall of 2013 as a dual enrolled student. In August 2016 he received his Master of Science degree in Metallurgical Engineering from Missouri University of Science and Technology.

As a student, Andrew interned in both the foundry and steel industries. He interned at Neenah Foundry in Neenah, WI and at US Steel in Granite City, IL. He was also involved in student organizations such as, the American Foundry Society and Alpha Sigma Mu.